

ADA Notice
 For individuals with sensory disabilities, this document is available in alternate formats. For information call (916) 654-6410 or TDD (916) 654-3880 or write Records and Forms Management, 1120 N Street, MS-89, Sacramento, CA 95814.

| | | |
|---|------------------------------------|---|
| 1. REPORT NUMBER CA18-2861 | 2. GOVERNMENT ASSOCIATION NUMBER | 3. RECIPIENT'S CATALOG NUMBER |
| 4. TITLE AND SUBTITLE <i>Prequalifying Testing Protocol for Buckling-Restrained Braces Applied to Steel Truss Bridges</i> | 5. REPORT DATE January 2018 | |
| 7. AUTHOR Joel Lanning, Muslim Abdulhusin Abdulkarim | | 6. PERFORMING ORGANIZATION CODE |
| 9. PERFORMING ORGANIZATION NAME AND ADDRESS Department of Civil and Environmental Engineering 800 N. State College Blvd California State University Fullerton, CA 92831 | | 8. PERFORMING ORGANIZATION REPORT NO. |
| 12. SPONSORING AGENCY AND ADDRESS California Department of Transportation Division of Engineering Services / SPI 1801 30th Street, MS #9-2/5i Sacramento, CA 95816 | | 10. WORK UNIT NUMBER |
| 15. SUPPLEMENTARY NOTES | | 11. CONTRACT OR GRANT NUMBER 65A0581 |
| 16. ABSTRACT | | 13. TYPE OF REPORT AND PERIOD COVERED Final Report |
| 17. KEY WORDS Buckling-Restrained Brace, BRB, Steel Truss Bridges, Testing Protocol, Loading Protocol | | 14. SPONSORING AGENCY CODE |
| 19. SECURITY CLASSIFICATION (of this report) None | | 20. NUMBER OF PAGES 84 |
| 21. COST OF REPORT CHARGED | | |

16. ABSTRACT

Buckling-restrained braces (BRBs) have become popular as ductile seismic force-resisting elements in building structures. This is due in part to a comprehensive design guide for BRB frames and a substantiated component prequalifying test loading protocol provided in the AISC Seismic Provisions for Structural Steel Buildings (AISC 2016). The test protocol represents, in a statistical sense, the demands on a BRB within a frame across a range of typical building sizes subjected to far-field ground motion. Even though BRBs have been utilized on a few bridges in the U.S. and Japan, there is no such BRB design procedure for use on bridges and only one prequalifying loading protocol has been developed. However, this protocol represents BRB demands from a suspension bridge subjected to near-fault ground motions. Therefore, this existing protocol is too specific and is perhaps overly conservative for most bridge BRB applications.

This work explored the development of a BRB prequalifying test loading protocol which represents brace demands within steel truss bridges, a more conventional bridge type, subjected to far-field ground motions. Two steel truss bridge models varying in truss configuration, span size, and number of spans were investigated for hypothetical seismic retrofit using BRBs as replacements for truss members identified as failing during a design-level earthquake. A parametric approach was then used to determine the BRB sizes and configurations. However, for one of these bridges no benefit to seismic performance was found despite the wide variety of BRB schemes and parameters explored. The other bridge exhibited a large reduction in the number of failed truss members due to the stable cyclic yielding ability the BRBs.

The retrofitted bridge model was then subjected to a suite of scaled far-field ground motions generating BRB demand time-histories used to construct a new loading protocol for BRB application within steel truss bridges. The resulting protocol exhibited inelastic characteristics similar to but less demanding than the AISC Protocol for BRBs within buildings. Given the wide-spread use of the AISC Protocol to prequalify many existing BRB component designs, the AISC protocol would ideally be applicable for BRB steel truss bridge implementation. However, since this work considered demands from only one bridge, further study on multiple truss bridges is required for this recommendation to apply to steel truss bridges in general. Future work should address this by applying the methodology to a wide range of bridges and seismic hazards to provide designers the crucial tool of a protocol applicable to all BRBs in steel truss bridges

17. KEY WORDS

Buckling-Restrained Brace, BRB, Steel Truss Bridges, Testing Protocol, Loading Protocol

18. DISTRIBUTION STATEMENT

No restrictions.
 This document is available to the public through the National Technical Information Service, Springfield, Virginia 22161

19. SECURITY CLASSIFICATION (of this report)

None

20. NUMBER OF PAGES

84

21. COST OF REPORT CHARGED

DISCLAIMER

This document is disseminated in the interest of information exchange. The contents of this report reflect the views of the authors who are responsible for the facts and accuracy of the data presented herein. The contents do not necessarily reflect the official views or policies of the State of California or the Federal Highway Administration. This publication does not constitute a standard, specification or regulation. This report does not constitute an endorsement by the California Department of Transportation of any product described herein.

For individuals with sensory disabilities, this document is available in Braille, large print, audiocassette, or compact disk. To obtain a copy of this document in one of these alternate formats, please contact: The Division of Research and Innovation, MS-83, California Department of Transportation, P.O. Box 942873, Sacramento, CA 94273-0001.

Prequalifying Testing Protocol for Buckling-Restrained Braces Applied to Steel Truss Bridges

by

Joel Lanning

Assistant Teaching Professor
University of California, Irvine
Civil and Environmental Engineering

Muslim Abdulhusin Abdulkarim

Graduate Student Researcher
California State University, Fullerton
Civil and Environmental Engineering

Final Report Submitted to the California Department of Transportation
under Contract No. 65A0581

ACKNOWLEDGEMENTS

Funding for this research was provided by the California Department of Transportation under Contract No. 65A0581 with Dr. Charly Sikorsky as the project manager. Thanks also goes to Tony Sánchez of Moffatt & Nichol for his advice on selecting bridge structures for this study and for providing resources towards the construction of the analytical models.

ABSTRACT

Buckling-restrained braces (BRBs) have become popular as ductile seismic force-resisting elements in building structures. This is due in part to a comprehensive design guide for BRB frames and a substantiated component prequalifying test loading protocol provided in the AISC Seismic Provisions for Structural Steel Buildings (AISC 2016). The test protocol represents, in a statistical sense, the demands on a BRB within a frame across a range of typical building sizes subjected to far-field ground motion. Even though BRBs have been utilized on a few bridges in the U.S. and Japan, there is no such BRB design procedure for use on bridges and only one prequalifying loading protocol has been developed. However, this protocol represents BRB demands from a suspension bridge subjected to near-fault ground motions. Therefore, this existing protocol is too specific and is perhaps overly conservative for most bridge BRB applications.

This work explored the development of a BRB prequalifying test loading protocol which represents brace demands within steel truss bridges, a more conventional bridge type, subjected to far-field ground motions. Two steel truss bridge models varying in truss configuration, span size, and number of spans were investigated for hypothetical seismic retrofit using BRBs as replacements for truss members identified as failing during a design-level earthquake. A parametric approach was then used to determine the BRB sizes and configurations. However, for one of these bridges no benefit to seismic performance was found despite the wide variety of BRB schemes and parameters explored. The other bridge exhibited a large reduction in the number of failed truss members due to the stable cyclic yielding ability the BRBs.

The retrofitted bridge model was then subjected to a suite of scaled far-field ground motions generating BRB demand time-histories used to construct a new loading protocol for BRB application within steel truss bridges. The resulting protocol exhibited inelastic characteristics similar to but less demanding than the AISC Protocol for BRBs within buildings. Given the widespread use of the AISC Protocol to prequalify many existing BRB component designs, the AISC Protocol would ideally be applicable for BRB steel truss bridge implementation. However, since this work considered demands from only one bridge, further study on multiple truss bridges is required for this recommendation to apply to steel truss bridges in general. Future work should address this by applying the methodology to a wide range of bridges and seismic hazards to provide designers the crucial tool of a protocol applicable to all BRBs in steel truss bridges.

TABLE OF CONTENTS

| | |
|---|------------|
| ACKNOWLEDGEMENTS | III |
| ABSTRACT..... | IV |
| TABLE OF CONTENTS | I |
| LIST OF FIGURES | II |
| LIST OF TABLES..... | IV |
| 1. INTRODUCTION | 1 |
| 1.1. Background..... | 1 |
| 1.2. Research Objective and Scope..... | 2 |
| 2. BUCKLING-RESTRAINED BRACES AND LOADING PROTOCOLS..... | 3 |
| 2.1. History | 3 |
| 2.2. Loading Protocols..... | 3 |
| 2.3. BRB on Bridges | 4 |
| 3. BRIDGE MODELING AND GROUND MOTIONS | 11 |
| 3.1. Bridges and Models | 11 |
| 3.2. Ground Motion Selection..... | 14 |
| 4. BRIDGE BRB PARAMETRIC DESIGN..... | 30 |
| 4.1. Identification of BRB Locations..... | 30 |
| 4.2. BRB Parameterization | 31 |
| 4.3. Parametric Analysis Results | 32 |
| 5. PROTOCOL DEVELOPMENT | 40 |
| 5.1. Protocol Characteristics | 40 |
| 5.2. Protocol Analysis..... | 41 |
| 6. SUMMARY AND RECOMMENDATIONS..... | 47 |
| 6.1. Summary of Analyses and Results | 47 |
| 6.2. Protocol Recommendations | 47 |
| 6.3. Recommendations for Future Work | 50 |
| REFERENCES..... | 52 |
| APPENDIX..... | 54 |

LIST OF FIGURES

| | |
|---|----|
| Figure 2.1 Buckling-Restrained Braces | 6 |
| Figure 2.2 Typical BRB Frames within a Building Structure..... | 6 |
| Figure 2.3 Response Data used in Developing the AISC BRB Loading Protocol (Sabelli, et al., 2003) | 7 |
| Figure 2.4 Layout of the added BRB to the Auburn-Foresthill bridge, and corresponding AISC protocol (developed for buildings) used for testing..... | 7 |
| Figure 2.5 BRBs on Japanese Bridges (Kanaji et al., 2006)) | 8 |
| Figure 2.6 Ductile end diaphragm using BRB experimental setup by Carden et al. 2004. | 8 |
| Figure 2.7 Ductile end diaphragm schemes studied by Celik et. al. 2009 | 9 |
| Figure 2.8 BRBs Used as Ductile Diaphragm (Japan) | 9 |
| Figure 2.9 Loading Protocol Development process (Lanning et al. 2013)..... | 10 |
| Figure 3.1 Location of Two Steel Truss Bridges | 23 |
| Figure 3.2 Klamath River Bridge | 23 |
| Figure 3.3 San Luis Ray Bridge from As-Built Drawing (Caltrans) | 24 |
| Figure 3.4 San Luis Ray Bridge As-Built Pier Layout | 25 |
| Figure 3.4 BRB Bilinear Model with Kinematic Hardening Rule..... | 25 |
| Figure 3.5 Typical BRB Hysteretic Behavior from Testing (Newell et al. 2003)..... | 25 |
| Figure 3.6 Design Response Spectra and Bridge Spectral Ordinates at the Fundamental Period | 26 |
| Figure 3.7 Ground Motion Suite Scaling Concept..... | 26 |
| Figure 3.8 Spectra Combination Methods for Determining Ground Motion Scaling Factor | 26 |
| Figure 3.9 Klamath River Bridge Design Motion Spectra..... | 27 |
| Figure 3.10 Klamath River Bridge Design Motion (See Table 3.3)..... | 27 |
| Figure 3.11 San Luis Ray River Bridge Design Motion Spectra..... | 28 |
| Figure 3.12 San Luis Ray River Bridge Design Motion (See Table 3.4) | 28 |
| Figure 3.13 Klamath River Bridge Ground Motion Suite Spectral Summary | 29 |
| Figure 3.14 San Luis Ray River Bridge Ground Motion Suite Spectral Summary | 29 |
| Figure 4.1 Original Truss Member Failing under Design Motion, Klamath River Bridge | 37 |
| Figure 4.2 Original Truss Member Buckling under Design Motion, San Luis Ray River Bridge | 37 |
| Figure 4.3 Location of BRB, Klamath River Bridge | 38 |

| | |
|---|----|
| Figure 4.4 Location of BRB, San Luis Ray River Bridge | 38 |
| Figure 4.5 Example KRB BRB Response under Design Ground Motion, Varied γ Value | 39 |
| Figure 5.1 Examples of BRB Responses from KRB Ground Motion Suite..... | 43 |
| Figure 5.2 KRB Suite BRB Statistical Summary of Rainflow Excursion Counting | 44 |
| Figure 5.3 KRB Loading Protocol for BRB | 45 |
| Figure 5.4 KRB Suite Statistical Summary of Cumulative Ductility, BRB B5 Location | 45 |
| Figure 5.5 KRB Loading Protocol for BRB | 45 |
| Figure 5.6 Comparison of KRB and AISC BRB Protocols | 46 |
| Figure 5.7 Comparison of the Cumulative Ductility Distribution of KRB and AISC BRB Protocols | 46 |
| Figure A.1 Klamath River Bridge Ground Motion Suite Time Histories and Spectra..... | 54 |
| Figure A.2 San Luis Ray Bridge Ground Motion Suite Time Histories and Spectra..... | 65 |

LIST OF TABLES

| | |
|--|----|
| Table 3.1 Klamath Bridge Model Modal Properties..... | 19 |
| Table 3.2 San Luis Ray Bridge Model Modal Properties..... | 20 |
| Table 3.3 Klamath River Bridge Ground Motion Suite..... | 21 |
| Table 3.4 San Luis Ray River Bridge Ground Motion Suite..... | 22 |
| Table 4.1 Summary of Parametric Study for BRB Design, Klamath River Bridge | 35 |
| Table 4.2 San Luis Ray Bridge Transverse Truss Member Properties..... | 36 |
| Table 4.3 Summary of Parametric Study for BRB Design, San Luis Ray Bridge..... | 36 |
| Table 4.4 Representative Transverse Truss End Frame Stiffnesses, San Luis Ray Bridge | 36 |
| Table 5.1 Absolute Maximum BRB Deformation Statistics, Klamath River Bridge Suite..... | 42 |

1. INTRODUCTION

1.1. Background

Application of energy dissipation devices on civil structures is well documented, increasingly popular and effective. For bridges in particular, viscous dampers and base isolation devices have been the dominate method of seismic protection. Meanwhile, a type of displacement-based metallic damper, called buckling-restrained braces (BRBs), have become popular in the past few decades as a ductile seismic force-resisting element in building structures (Uang et al., 2004, and Xie et al., 2005).

Their rise in use is due in part to a comprehensive guide to the design of BRB frames (BRBFs) and a substantiated set of prequalifying testing criteria for BRBs, provided in the AISC Seismic Provisions for Structural Steel Buildings (AISC 2016). The testing criteria includes a loading protocol for prequalifying physical testing of BRBs, which is meant to prove that component designs are capable of performing as expected during design-level seismic events. The cycles within the protocol represent, in a statistical sense, the demands on a BRB within a building frame found using a range of typical building sizes subjected to far-field ground motion. Many such BRB prequalifying testing programs have been conducted such as those by Newell et al., (2005), Kim et al. (2009), and Lanning et al. (2012).

Even though a few bridges in the U.S. and Japan have been retrofitted with BRB, relatively very little bridge-specific BRB research has been conducted. Therefore, no established design criteria have been developed nor has a testing protocol been developed that is applicable to a wide variety of bridges. Advancing the adoption of BRB into the bridge design industry requires further investigation into these prequalifying loading protocols. Without this knowledge engineers are forced to either assume a loading protocol or use that provided by AISC. The former is essentially a random loading sequence which may have no clear relationship to the actual behavior of the bridge under consideration. The latter is not necessarily appropriate for bridge structures because it was developed using buildings, not bridges. Therefore, both options are a questionable metric for BRB performance within bridge structures subjected to earthquake ground motion.

1.2. Research Objective and Scope

The original intent of this work was to provide Caltrans with a *comprehensive* set of loading protocols for prequalification of BRBs to be used on conventional bridges. This included four primary objectives: (i) identify bridge types and BRB configurations that would serve a benefit in terms of seismic performance; (ii) designing and modeling these selected bridges and (iii) perform nonlinear time-history analyses in order to generate data to form proposed prequalifying loading protocols. Finally, (iv) make a set of recommendations regarding inclusion of the protocols into the Seismic Design Specifications for Steel Bridges.

Through discussions with Caltrans it was deemed more pertinent to isolate one specific bridge type and steel truss bridges were identified to be studied herein. Two such bridges were identified, and as-built drawings were provided to the authors by Caltrans and Moffatt & Nichol. Therefore, this report summarizes work on objectives (ii), (iii), and (iv) above.

More specifically, the scope of this report includes: (1) the construction of two steel truss bridge finite element models, (2) selection of a suite of ground motions scaled to represent design-level earthquakes applied to each model, (3) summary of a parametric design process carried out to identify the size and configuration of BRBs on each bridge, (4) the development of a prequalifying test loading protocol considering the BRB deformational demands collected from the application of these motions, (5) recommendations about the usefulness and applicability of the developed protocol, as well as limitations, and (6) a description of suggested future work of which this study is only a small part.

2. BUCKLING-RESTRAINED BRACES AND LOADING PROTOCOLS

2.1. History

Buckling-restrained braces (BRBs) originally developed in the 1970s in Japan but did not gain acceptance in buildings until after the 1995 Kobe Earthquake. This was in an effort to design “damage-tolerant” structures (Wada et al., 2004). These braces dissipate energy, and relieve critical portions of the building from damage, by yielding through both tension and compression as shown Figure 2.1(a). A restraining member, typically a steel tube sleeve filled with mortar as shown in Figure 2.1(b), allows the steel core to yield in compression without buckling. A typical buckling-restrained braced frame (BRBF) in a building structure is shown in Figure 2.2. Connections can be welded, bolted, or pinned.

Recently, BRBs have become popular as a ductile seismic force-resisting element in building structures (Uang et al., 2004) due in part to a comprehensive guide to the design of BRBF and a substantiated set of prequalifying testing criteria for BRBs, provided in the AISC Seismic Provisions for Structural Steel Buildings (AISC 2010). The testing criteria includes physical testing of BRBs to a loading protocol that was developed using brace demands obtained from various braced frame buildings. Many private and proprietary BRB prequalifying testing programs have been conducted such as those by Newell et al., (2005), Kim et al. (2009), and Lanning et al. (2012).

2.2. Loading Protocols

Cyclic loading protocols for testing the seismic performance of structural components should assess the capability of surviving statistically derived earthquake demands expected for a specific structure type and component configuration (Krawinkler et al., 1983, 2009). Generally, this is achieved by subjecting a number of representative structural models to a set of ground motions which constitute a certain level of seismic risk. The simulated component responses are collected, analyzed, and then used to formulate a simplified, representative, and statistically significant demand time history. The resulting protocol should replicate a reasonably conservative cumulative damage that is expected for the specific structural component (Krawinkler et al., 1992).

Following this convention, the AISC 341, seismic provisions for steel buildings, contains cyclic loading protocols specific to various structural steel systems. One such protocol is for

buckling-restrained braces, which was mainly developed from the work conducted by Sabelli et al., in 2003. Figure 2.3 contains an example summary of frame deformations from the study (which can be translated to BRB demands) for the suite of design-level-scaled earthquakes used. A number of different building models, with BRB frames, were analyzed and the resulting demands were incorporated together to form the AISC 341 BRB Prequalifying Loading Protocol, shown in Figure 2.4(c). This provides a robust testing sequence which effectively considers the statistical BRB demands from several buildings and many seismic events. Hence, it is a conservative metric for accepting a prototype BRB as capable of performing its crucial role as a structural fuse within a building frame during a seismic event.

2.3. BRB on Bridges

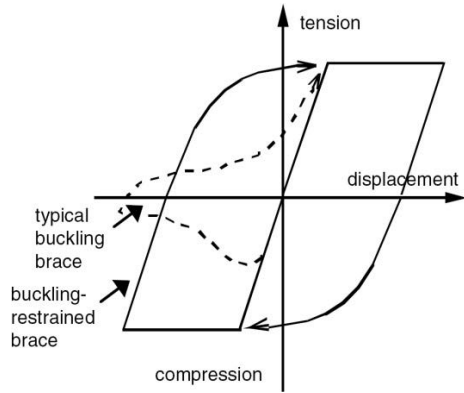
Very limited research has addressed the use of BRB on bridges. Therefore, the applications and potential beneficial configurations have not been fully developed. One of the only U.S. bridge projects to incorporate BRBs is summarized by Reno and Pohll (2010). The Auburn-Foresthill Bridge included the installation of several BRBs as force- and displacement-limiting members attached to the abutments, as shown in Figure 4. However, this project adopted the AISC protocol, in Figure 2.4(c), which was developed to represent the far-field BRB demands within buildings, not bridges. This exhibits the need for bridge-specific protocols and analytical study of BRBs on bridges for U.S. bridges.

Japanese engineers have also applied BRBs to bridges, but again, without developing statistically relevant protocols. The Owatari Bridge was constructed with BRBs as truss members and in portal frames as ductile bracing elements (Ge et al. 2008). Usami et al. (2005) summarized the design efforts, and benefits, involved in retrofitting a Japanese steel arch bridge, shown in Figure 2.5, using BRBs to limit forces imparted to the foundation and surrounding structure. Cardin et al. (2004), Figure 2.6, along with Celik and Brunea (2009), Figure 2.7, both studied the performance and effects of BRB applied as ductile end diaphragm braces. A similar ductile diaphragm design has been used in Japan, as shown in Figure 2.8. Other configurations have been studied, but no use-specific testing protocols have been developed.

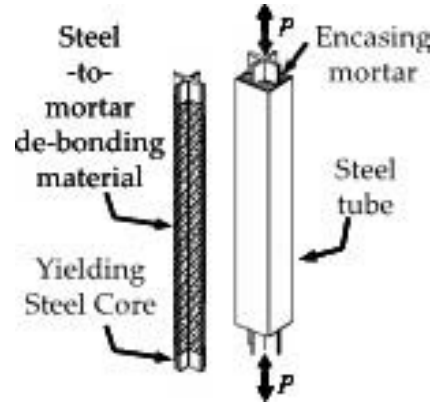
Most recently Lanning et al. (2011) studied the feasibility and showed the benefit of using BRB on the Vincent Thomas Bridge as a replacement of existing viscous dampers. The analyses permitted development of a loading sequence, shown in Figure 2.9, representative of the simulated

demands, which then permitted physical testing. These tests provided strong evidence that BRBs are very capable of sustaining the inelastic cyclic demands required to mitigate long-span bridge seismic response due to strong near-fault ground motions. (Lanning et al., 2013). This study represents a model process for advancing the use of BRBs on bridges; analysis results were used to generate a loading protocol that statistically represents the demands of a BRB within a structure, which is then applied through physical testing to prove the brace performance. This process facilitates a standard for codification, which enables designers to use BRBs in bridge designs.

The 2nd edition of the Caltrans Seismic Design Specifications for Steel Bridges (Caltrans 2016), or Caltrans SDS, contains the first set of guidelines on the use of BRBs on bridges in the U.S. (Lanning et al. 2014). The recommendations have been derived from the study described above. This protocol is fairly conservative since it represents the 84th percentile demand from a suite of near-fault ground motions scaled to one design spectrum applied to only one bridge, the Vincent Thomas Bridge. Therefore, it represents a narrow range of earthquake intensities. Therefore it is most likely unreasonably conservative for other types of less flexible bridges (i.e., having less displacement demands) and certainly too conservative for any which are not located near a major fault line. Therefore, an expanded effort is required to develop a set of bridge-BRB prequalifying loading protocols that more appropriately cover a number of different bridge structures, brace schemes, and seismic demands (i.e., design-level and maximum considered events). This study takes on one such bridge type, steel truss bridges.



(a) Hysteretic Behavior:
BRB vs. Conventional Brace
(Clark et al. 1999)



(b) Anatomy of BRB

Figure 2.1 Buckling-Restrained Braces



Figure 2.2 Typical BRB Frames within a Building Structure

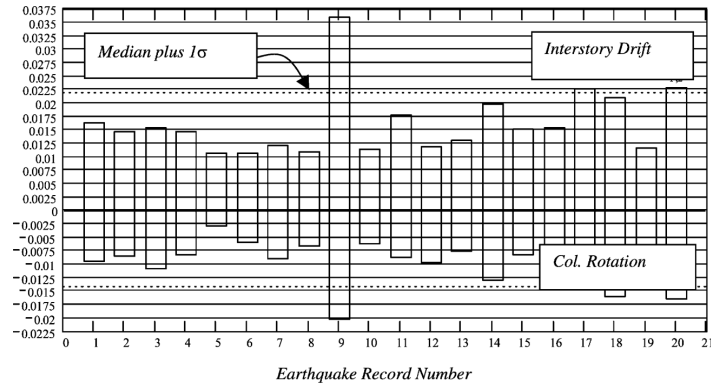
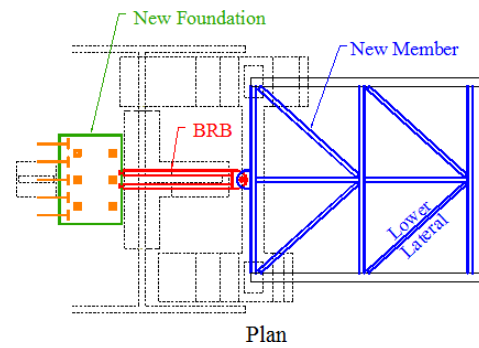


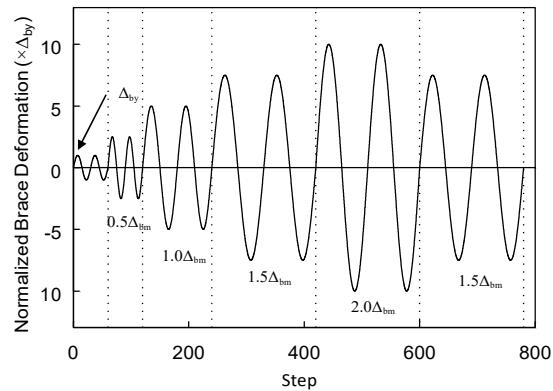
Figure 2.3 Response Data used in Developing the AISC BRB Loading Protocol (Sabelli, et al., 2003)



(a) Fuse member



(b) Layout of new BRB

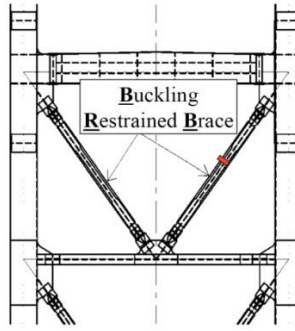


(c) AISC Protocol

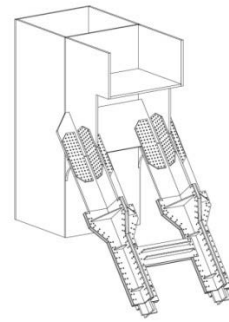
Figure 2.4 Layout of the added BRB to the Auburn-Forest Hill bridge, and corresponding AISC protocol (developed for buildings) used for testing



(a) Minato Bridge



(b) Minato Bridge Tower BRBs



(c) Minato BRB End Connections



(d) Owatari Bridge exhibits BRBs in several locations

Figure 2.5 BRBs on Japanese Bridges (Kanaji et al., 2006))



Figure 2.6 Ductile end diaphragm using BRB experimental setup by Carden et al. 2004.

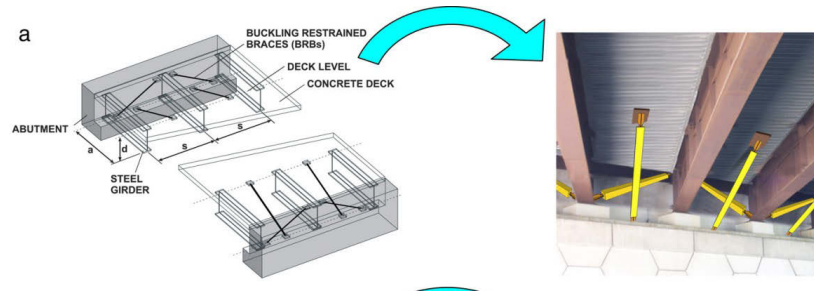
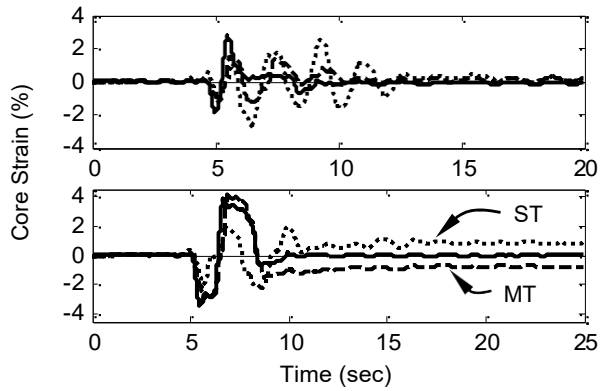


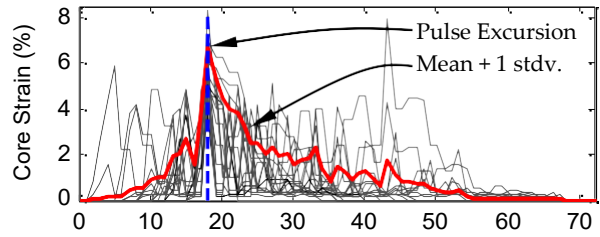
Figure 2.7 Ductile end diaphragm schemes studied by Celik et. al. 2009.



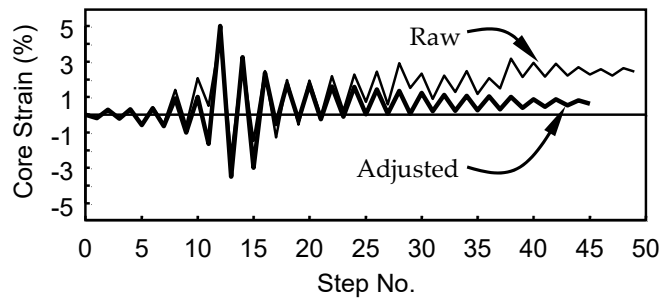
Figure 2.8 BRBs Used as Ductile Diaphragm (Japan)



(a) Example Vincent Thomas Bridge BRB Core Strain Time Histories



(b) Example of Pulse-Aligned Inelastic Excursions



(c) Near Fault Protocol, 2nd edition Caltrans SDS

Figure 2.9 Loading Protocol Development process (Lanning et al. 2013)

3. BRIDGE MODELING AND GROUND MOTIONS

3.1. Bridges and Models

Two steel arch bridges were identified as candidates for BRB retrofit study. The Klamath River Bridge (KRB) and the San Luis Ray River Bridge (SLRB) located in Northern and Southern California, respectively. As shown in Figure 3.1, they represent bridges built for very different locations, and presumably designed to withstand somewhat different seismic demands. However, each bridge was built many decades ago, with KRB having been constructed around 1930 and SLRB in the 1950s. Together with no original design calculations available the exact design philosophy was unknown. This was not a critical problem as the bridge geometries and dynamic properties were the structural aspects needed to convey the general seismic demands imparted to the components of the trusses members. This was not ideal but nonetheless unavoidable for the project. Further, the Caltrans inventory of steel truss bridges is aged as this bridge type is not common in contemporary construction practices in California. Even still the results provide new insight into the seismic demands that can be expected to be imparted to BRBs on steel truss bridges.

The finite element software CSi-Bridge (CSi 2016) was used to model the bridges. This software is a nonlinear analysis finite element package tailored for structural modeling of bridge structures and is widely used in industry. Therefore, it permitted the modeling of these large bridge structures which included member nonlinear material behavior including the representation of BRBs, to a degree sufficient for this study as discussed below, and for the study of the potential buckling of existing lateral truss members discussed in Section 4.1. Further, CSi-Bridge was able to carry out nonlinear time history analyses appropriate for this study, which required simulating steel yielding while the models were subjected to ground acceleration time history input.

Klamath River Bridge (KRB)

The KRB is a deck truss bridge that carries CA 96 across the Klamath River in Humboldt County California constructed circa 1930. The bridge consists of three spans with a total length 540 ft, with a main arched span of approximately 290 ft. An elevation of the bridge is shown in Figure 3.2(a). The bridge has two concrete piers, supported by large footings, with somewhat different heights; one stands approximately 58 ft. and the other around 70 ft. The truss members can be divided into two primary groups main span truss members, carrying the roadway and mostly consisting of built-up sections, and lateral truss members, connected to the main truss members by

gusset plates and are generally smaller sections. The bridge has six vertical lateral bracing trusses in 12 locations along the span. These vertical trusses comprise of two different steel angle sections and all are connected together by gusset plates and are in a chevron braced frame configuration as shown in Figure 3.2(a). The transverse truss along the span is configured in a similar fashion, composed of rolled and built up members, and is displayed on the bridge model 3D-view in Figure 3.2(b). The deck is carried by stringers and floor beams which are framed into the panel points of the main vertical truss. Due to the era in which the bridge was constructed, the nominal steel yield strength is 30 ksi.

San Luis Ray River Bridge (SLRB)

The SLRB, built in 1949, is also a deck truss bridge which carries the Coast Highway, CA Route 1, across the San Luis Ray River in Oceanside, CA., adjacent to the I-5 freeway. An elevation of the bridge is shown in Figure 3.3(a). The three truss spans, each approximately 265 ft in length, are supported on concrete piers atop pile caps as well as concrete abutments at either end of the bridge. The main truss members are, again, built-up sections while rolled sections make up the lateral trusses as well as many of the transverse vertical trusses. The transverse vertical trusses are configured in a lattice type frame, as can be observed in Figure 3.3(a) and (b). The bottom transverse truss along the span is configured in an x-pattern, composed of rolled and built up members, and is best displayed using the bridge model 3D-view in Figure 3.3(b). Again, the steel available at the time of bridge construction had nominal yield strength of 30 ksi.

Bridge Modeling

Since both bridges are of similar steel truss construction, each bridge was modeled in essentially the same manner. Referencing a partial set of as-built drawings, provided by Caltrans, bridge member cross sectional properties were modeled either directly using the CSi-Bridge section library or, in the frequent case of the use of built-up sections on this older bridge, through assignment of equivalent section properties. Truss member ends were released from carrying moment, while stringers and floor beams were assigned as either continuous or simply supported beams as necessary.

Bridge concrete decks were modeled as 4-node shell elements, connected to the floor beams and stringers with no joint releases. Shell elements were assigned a Young's modulus of the representative of reinforced concrete, $E = 3,600$ ksi, and a membrane thickness equal to the existing slab thickness. Shell bending thickness was neglected as the out-of-plane bending stiffness

of the deck was not considered significant for this study. The partial as-built drawings did not explicitly detail composite floor beams and stringers; however, composite action was assumed. It was deemed that this method of deck modeling should sufficiently represent the composite action between the bridge deck and the floor beams and stringers. Regardless, as discussed below, the bridge deformation most affected by composite action was not of primary concern for this study; rather the transverse direction was most important. Additionally, an expansion joint provided between each span was not modeled explicitly in the SLRB.

The abutments of each bridge were assigned simple supports (i.e., not fixed) since approach spans were not embedded into the abutments, and abutments were provided as basic vertical supports. Further, one end of the approach span was free to travel in the bridge longitudinal direction since the bridge spans are supported on rocker supports to accommodate thermal expansion and contraction (i.e., overall bridge longitudinal restraint is not present in the real structure). Bridge piers were assumed to be fixed at their bases because they were either cast on large footers or, as is the case for SLRB interior piers, on large pile caps. Piers and associated members were assigned as beam elements with all geometric properties (e.g., cross sectional area, moment of inertia) found from the as-built drawings. For instance, the SLRB piers and caps were modeled as separate beams with simple connections receiving the trusses. In both bridge models, links were used to constrain pier nodes to make the pier and pier cap act as one element since this should be consistent with the cast-in-place construction. The configuration of the SLRB pier model is shown in Figure 3.4, schematically.

Often in bridge modeling, piers will have support conditions which represent the soil or bedrock conditions (a support matrix). Not only was the information not readily available, but this level of detail was deemed inappropriate for this study which is principally focused on the interaction between the superstructure, substructure and BRBs. However, the soil site class for each bridge was considered in the ground motion selection, as discussed in Section 3.2.

The assignment of bridge mass for dynamic and modal analyses was provided by directly allocating material densities to each model element. Therefore, the distribution of mass in the models should be realistic and, as shown below, with reasonable modal periods the dynamic behavior of the bridges was deemed to be sufficiently accurate for the purposes of this study. Finally, damping of the models for dynamic time history analyses was provided using the Rayleigh damping method coefficients resulting in damping equal to 3% of critical in modes 1 and 3.

Bridge Model Modal Analysis

Modal properties of the KRB and SLRB models are presented in Table 3.1 and Table 3.2, respectively. Not all modes are shown for brevity, but mostly because after some preliminary (and diagnostic) analyses it was clear that only the lateral truss structures were suitable for investigating their replacement with BRBs. Therefore, the significant modes were deemed to be those making up transverse modal mass participation of around 80-90%. Within this range of periods a reasonable amount of vertical mode participation was also captured. This information was critical for the selection and scaling of ground motion records. The first transverse mode of the SLRB is potentially somewhat too long. However, no modeling errors could be identified and without any further independent analysis or comparisons the model was considered sufficiently accurate for this study.

Buckling-Restrained Brace Modeling

A common BRB finite element model (Kim et al. 2003, Black et al. 2004, Ravi et al. 2007, Lanning et al. 2011, and Di Sarno et al. 2013, among others) was used for this project. A bilinear truss element with a kinematic cyclic hardening rule, shown in Figure 3.5(a), exhibits the basic cyclic response of typical BRBs. A comparison between this model and data taken from a typical BRB component test is shown in Figure 3.5(b). Modeling techniques do exist to more closely match BRB cyclic behavior and are now fairly commonly used. However, these merely capture a small additional amount of dissipated energy and are likely to account for a relatively minor difference in overall BRB demands and response in this work.

It should be noted that previous studies have shown this modeling approach is not sufficient for large BRB core strain values (beyond about 3%), nor does it represent well the cyclic behavior of BRBs with stainless steel cores (Lanning et al., 2014). However, large core strains were not expected (and were not observed) and BRB core materials other than A36 steel were not considered here. Therefore, the bilinear BRB model was deemed appropriate for this study.

3.2. Ground Motion Selection

When conducting time history analyses for seismic design of structures, digital recordings of ground motions are input to the finite element software for application to the structure. Further, the unpredictable nature of seismic motion necessitates the use of a number of ground motions for proper protocol development. Therefore, ground motions were selected and used for two primary

purposes; (i) a design earthquake was selected for conducting the BRB design process (See Chapter 4), then (ii) a suite of ground motions was selected for use in the development of a proposed prequalifying BRB loading protocol for steel truss bridges (See Chapter 5).

The Pacific Earthquake Engineering Research Center (PEER) Ground Motion Database NGA-West 2 (PEER NGA) was used as the source of ground motion time histories in this study. Care was taken to ensure that the earthquake records appropriately reflected the average shear wave velocity, V_{s30} , at the bridge sites, were consistent with far-field motion (6- to 200-mile rupture distance and no pulse characteristic) and were scaled to the given design-level Caltrans Acceleration Response Spectra (ARS) within the period range of interest of the structures. The ARS curves for each bridge are shown in Figure 3.7, where the first mode period for each bridge is shown for reference. The site soil conditions for KRB and SLRB, respectively, were considered as Type C (data was available to provide a value of $V_{s30} = 1,835$ ft/sec) and Type D ($V_{s30} = 600$ to 1,200 ft/sec).

Ground Motion Scaling

Ground motion scaling was performed using the online PEER database tool which provides a scaling factor for each ground motion record of interest within the database. The factor is found using a well-established and widely-used algorithm which minimizes the mean squared error (MSE) between a given target acceleration spectrum and that of each ground motion. This algorithm uses a scaling factor in the frequency domain, as shown in Figure 3.8 which is then directly applied to the acceleration time history.

The spectrum scaled by this factor is made up of a combination of the individual components recorded (i.e., two perpendicular horizontal components and a vertical component). The PEER online tool provides a number of methods for computing the combined spectrum. Since most seismic design studies are primarily focused on horizontal shaking, PEER offers several options which use only horizontal components in forming the representative spectrum with which to determine the scale factor. A typical combination method is the square root sum of squares (SSRS) method. This method was found to be inappropriate for this project since, as mentioned above, the primary direction of dynamic motion affecting the BRB locations within the bridges (also discussed in Chapter 4) was the transverse horizontal direction. As shown in Figure 3.9(a), when the horizontal components are combined using the SRSS they are, in effect, added together. This eventually misrepresents the transverse direction shaking, with respect to the target spectrum,

when applying the individual records in their respective directions to the bridge model. A more appropriate combination method is to combine the horizontal components using a geometric mean. The contrast between using the SSRS and the geometric mean can be observed in Figure 3.9. When the scaling factor considers the mean of the two horizontal components the transverse direction more closely matches the target spectrum and therefore correctly represents the expected seismic demand. Therefore, the geometric mean of the two horizontal components was used for scaling in this project.

Other combinations do exist such as the Complete Quadratic Combination (CQC) method. Although these methods may be applicable to this spectral combination problem, it is commonly used as a modal combination method for dynamic analyses and, most importantly, this method is not available through the PEER online tool. This is a critical distinction, because the PEER database has been developed by many expert researchers in the area of seismology and earthquake engineering for use by engineers and researchers conducting time history analyses for seismic design. Using a different scaling method (manually) is well beyond the scope of this work, and therefore the PEER tool is considered to be sufficient for ground motion selection and scaling.

The following section will discuss the last remaining scaling issue; careful consideration was paid to the spectral period range used in computing the scaling factor.

Design Motion and Protocol Motion Suite

As mentioned above, two primary tasks required the selection and scaling of ground motions; the parametric design of bridge BRBs and developing the BRB protocol both required ground motions to be scaled to be consistent with the corresponding design-level ARS for each bridge. Several published documents cover accepted methods of ground motion selection and scaling for time history analyses. The National Institute of Standards Technology (NIST) GCR 11-917-15 (NIST 2011) summarizes these requirements. The most relevant of these are from AASHTO LRFD Bridge Design Specification (AASHTO, 2010) and include the following (in addition to those more obvious criteria such as soil site class, already discussed here):

- 1) Records are to be scaled to the approximate level of the design response spectrum in the period range of significance.
- 2) A minimum of three records is to be used.
- 3) Each record should contain all three motion direction components.
- 4) Each record should represent a 7% probability of exceedance in 75 years, as is consistent with AASHTO seismic design level response spectrum.

- 5) If the number of records used is greater than three but less than seven, then design quantities (e.g., demands, displacements) are to be taken as the maximum response from the analyses.
- 6) If the number of records used is greater seven, then design quantities may be taken as the mean from the analyses.

Since the goal of this project is not to develop an actual retrofit or new seismic design using time history analyses, these rules do not necessarily apply. However, they are used as a guide in how to scale, the number of motions used, the relative strength of motions to be considered (design level versus maximum credible, etc.), and to what statistical level the results should be used (e.g. the mean or 84th percentile of demands).

Perhaps the most important item from the list above is to scale within with the significant period range. This range is somewhat subjective; however, it was determined that for this study the period range covering modes accounting for 80-90% of the participating mass in the transverse direction. But, as is evident from Table 3.1 and Table 3.2 this represents a very wide period range. Therefore, only the primary two transverse modes were used to determine the range considered for scaling computation. A weighing function in the PEER online tool is available to define custom period ranges to be included in the computation of the scaling factor, by way of minimizing the MSE.

Hence, for each bridge the first two primary modes representing at least 80% modal mass participation in the transverse direction were used with a weight proportional to their individual contributions to their combined modal mass participation. For example, the KRB modes 1 and 4 represented 69% and 16% transverse modal mass participation for a combined 85%. Therefore, mode 1 was assigned a weight of 0.81 ($= 69/85$) and a weight of 0.19 ($= 16/85$) was assigned to mode 4. So, the scaling factor was determined with a minimum MSE within period ranges that are directly applicable to the design task at hand. In other words, since the transverse direction was found to be critical, the influence of the target spectrum was emphasized in the determination of the overall scaling factor only with the primary transverse modal period ranges. Specifically, a 0.1 second period range around each transverse mode was used in the weight function (See

Ground motion suites are summarized in Table 3.3 and Table 3.4. The design motion was selected as having the smallest MSE, or nearly so, together with having one horizontal component spectral ordinate most nearly equal to that of the target (design) spectrum at the first transverse modal period. For the KRB this is displayed in Figure 3.10, with the corresponding ground motion

shown in Figure 3.11. Likewise, for the SLRB Figure 3.12 displays the design spectra for the design motion, and Figure 3.13 the ground motions.

Additionally, the location of the design earthquake event was considered as marginally important. Since these bridges are both in California, motions having occurred in California were given preference. As indicated in Table 3.3 and Table 3.4 the 1971 San Fernando record was used for both bridges as the design earthquake. This was coincidental, and the records are from different stations (RSN) and have very different scale factors which represent the different spectral requirements and very different modal properties of the two locations and bridges.

Additional aspects of the ground motions selected as the suite included picking those with the smallest scaling factor and MSE for a given event (i.e., if multiple recordings were available for the same event then a combination of the smallest MSE and scale factor indicated which particular record to use in the suite). A summary of the ground motion suite spectra, compared to the target (design) spectrum, is provided for each bridge in Figure 3.14 and Figure 3.15.

Table 3.1 Klamath Bridge Model Modal Properties

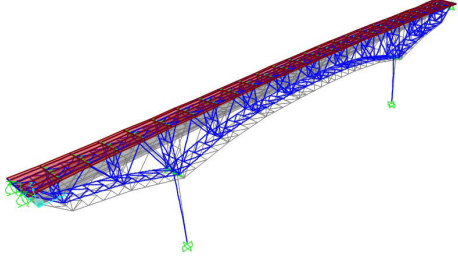
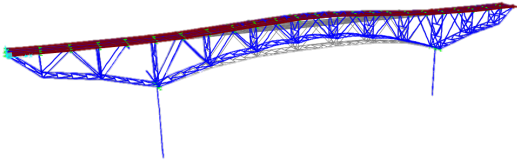
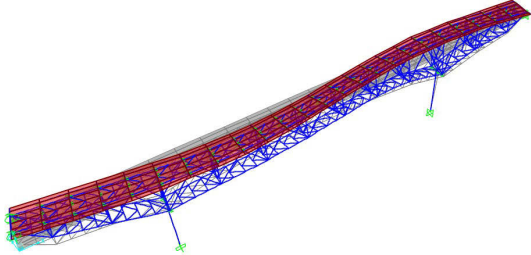
| Mode | Period (sec.) | Primary Modal Participating Mass Ratio | | Mode Shape |
|--|---------------|--|-------------------|--|
| | | % | Direction | |
| 1 | 1.032 | 69% | Transverse |  |
| 3 | 0.337 | 21% | Vertical |  |
| 4 | 0.289 | 16% | Transverse |  |
| Used in Ground Motion Scaling: Modes 1 and 4 account for 85% Transverse Participation | | | | |

Table 3.2 San Luis Ray Bridge Model Modal Properties

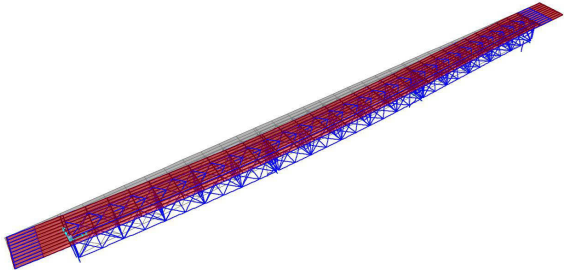
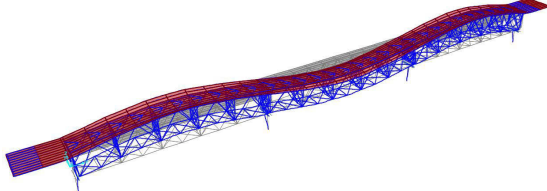
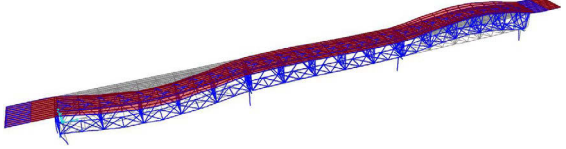
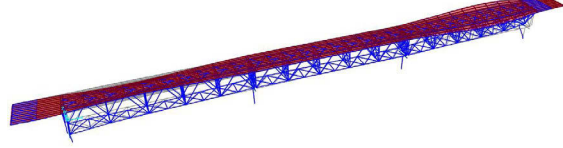
| Mode | Period (sec.) | Primary Modal Participating Mass Ratio | | Mode Shape |
|---|---------------|--|------------|--|
| | | % | Direction | |
| 1 | 2.39 | 75% | Transverse |  |
| 3 | 0.50 | 7% | Vertical |  |
| 5 | 0.45 | 12% | Transverse |  |
| 6 | 0.44 | 38% | Vertical |  |
| <p>Used in Ground Motion Scaling: Modes 1 and 5 account for 87% Transverse Participation</p> | | | | |

Table 3.3 Klamath River Bridge Ground Motion Suite

| Record No. | RSN | Event Name | Year | Mean Squared Error | Scale Factor | V_{s30} (m/s) |
|------------|-----------|-----------------------|-------------|--------------------|--------------|-----------------|
| 1 | 14 | Kern County | 1952 | 0.238 | 2.97 | 515 |
| 2 | 17 | Southern Calif | 1952 | 0.010 | 8.48 | 494 |
| 3 | 33 | Parkfield | 1966 | 0.211 | 1.89 | 528 |
| 4 | 50 | Lytle Creek | 1970 | 0.120 | 3.85 | 486 |
| 5 | 72 | San Fernando** | 1971 | 0.049 | 3.91 | 600 |
| 6 | 125 | Friuli Italy | 1976 | 0.038 | 1.36 | 505 |
| 7 | 135 | Santa Barbara | 1978 | 0.028 | 7.10 | 466 |
| 8 | 164 | Imperial Valley | 1979 | 0.041 | 2.22 | 472 |
| 9 | 216 | Livermore | 1980 | 0.020 | 5.17 | 650 |
| 10 | 231 | Mammoth Lakes | 1980 | 0.033 | 2.01 | 537 |
| 11 | 265 | Victoria Mexico | 1980 | 0.006 | 1.16 | 472 |
| 12 | 302 | Irpinia Italy | 1980 | 0.003 | 3.46 | 575 |
| 13 | 336 | Coalinga | 1983 | 0.005 | 4.03 | 542 |
| 14 | 472 | Morgan Hill | 1984 | 0.007 | 4.44 | 544 |
| 15 | 481 | Lazio-Abruzzo Italy | 1984 | 0.009 | 8.88 | 475 |
| 16 | 484 | Pelekanada Greece | 1984 | 0.539 | 3.14 | 528 |
| 17 | 501 | Hollister | 1986 | 0.050 | 5.28 | 609 |
| 18 | 512 | N. Palm Springs | 1986 | 0.069 | 5.36 | 531 |
| 19 | 554 | Chalfant Valley | 1986 | 0.003 | 5.26 | 537 |
| 20 | 587 | New Zealand | 1987 | 0.023 | 1.78 | 551 |
| 21 | 671 | Whittier Narrows | 1987 | 0.117 | 3.71 | 508 |
| 22 | 739 | Loma Prieta | 1989 | 0.059 | 1.79 | 489 |

* KRB site soil conditions considered as Type C (1,835 ft/sec), V_{s30} ranging 1,200 to 2,500 ft/sec

** Design ground motion used in Chapter 4.

Table 3.4 San Luis Ray River Bridge Ground Motion Suite

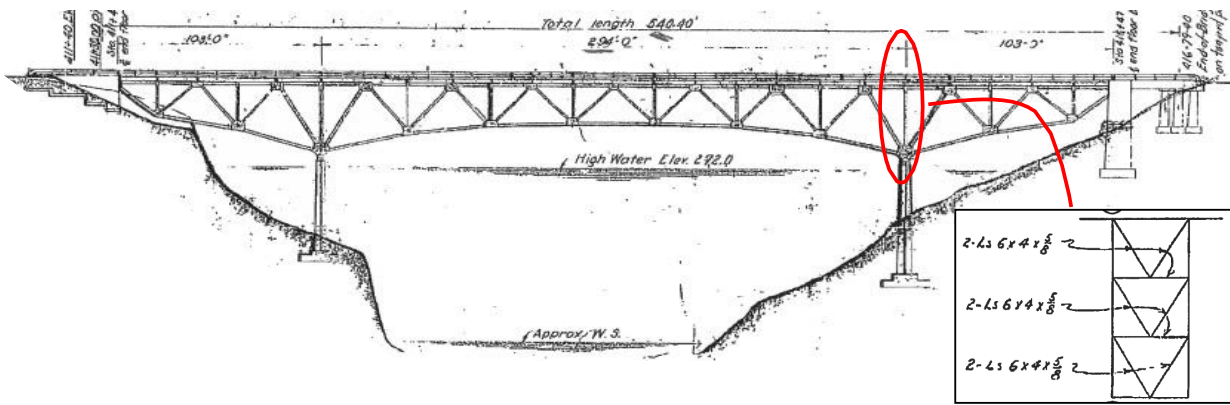
| Record No. | RSN | Event Name | Year | Mean Squared Error | Scale Factor | V_{s30} (ft/sec) |
|------------|-----------|------------------------|-------------|--------------------|--------------|--------------------|
| 1 | 8 | Northern Calif | 1941 | 0.752 | 7.63 | 718 |
| 2 | 9 | Borrego | 1942 | 0.097 | 7.67 | 699 |
| 3 | 11 | Northwest Calif (1951) | 1951 | 1.086 | 7.43 | 718 |
| 4 | 12 | Kern County | 1952 | 0.017 | 5.45 | 1,036 |
| 5 | 20 | Northern Calif (1954) | 1954 | 0.002 | 2.07 | 718 |
| 6 | 22 | El Alamo | 1956 | 0.161 | 7.88 | 699 |
| 7 | 26 | Hollister | 1961 | 0.184 | 4.07 | 653 |
| 8 | 31 | Parkfield | 1966 | 0.399 | 3.61 | 843 |
| 9 | 34 | Northern Calif | 1967 | 0.690 | 6.91 | 718 |
| 10 | 36 | Borrego Mountain | 1968 | 0.126 | 3.63 | 699 |
| 11 | 69 | San Fernando** | 1971 | 0.002 | 8.23 | 715 |
| 12 | 97 | Point Mugu | 1973 | 0.471 | 5.88 | 817 |
| 13 | 122 | Friuli Italy | 1976 | 0.066 | 5.00 | 817 |
| 14 | 141 | Tabas Iran | 1978 | 0.022 | 7.05 | 918 |
| 15 | 154 | Coyote Lake | 1979 | 0.265 | 5.03 | 1,102 |
| 16 | 175 | Imperial Valley | 1979 | 0.008 | 2.82 | 646 |
| 17 | 266 | Victoria Mexico | 1980 | 0.021 | 2.32 | 794 |
| 18 | 280 | Trinidad | 1980 | 0.085 | 8.09 | 1,023 |
| 19 | 312 | Taiwan SMART1 | 1981 | 0.148 | 6.27 | 1,030 |
| 20 | 314 | Westmorland | 1981 | 0.258 | 5.13 | 686 |
| 21 | 323 | Coalinga | 1983 | 0.024 | 7.22 | 1,178 |

* SLRB site soil conditions considered as Type D, V_{s30} ranging 600 to 1,200 ft/sec

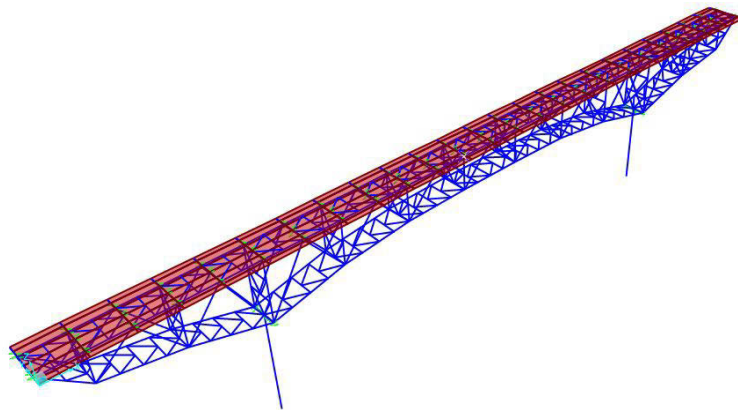
** Design ground motion used in Sec. 4



Figure 3.1 Location of Two Steel Truss Bridges

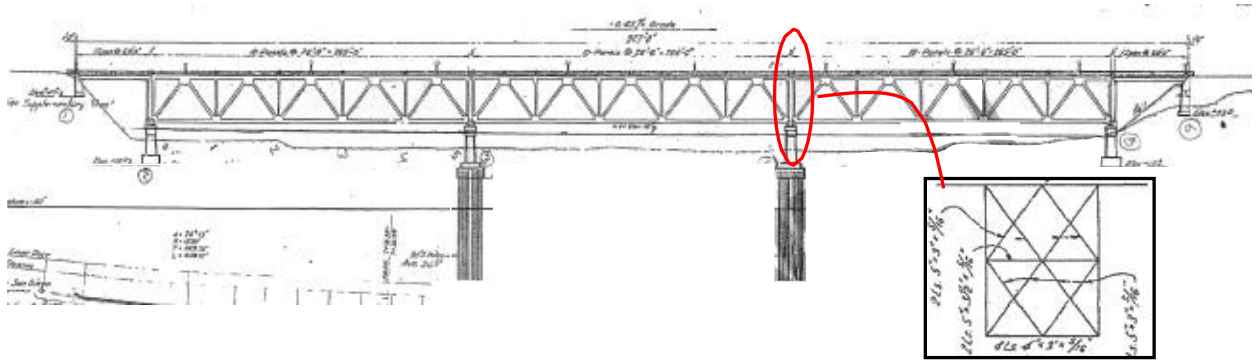


(a) Elevation from As-Built Drawing (Caltrans)

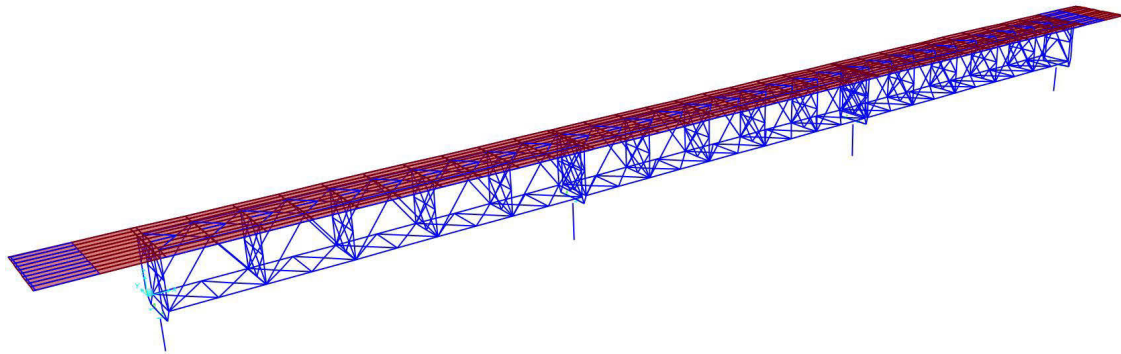


(b) CSI-Bridge Model

Figure 3.2 Klamath River Bridge



(a) Elevation from As-Built Drawing (Caltrans)



(b) CSI-Bridge Model

Figure 3.3 San Luis Ray River Bridge

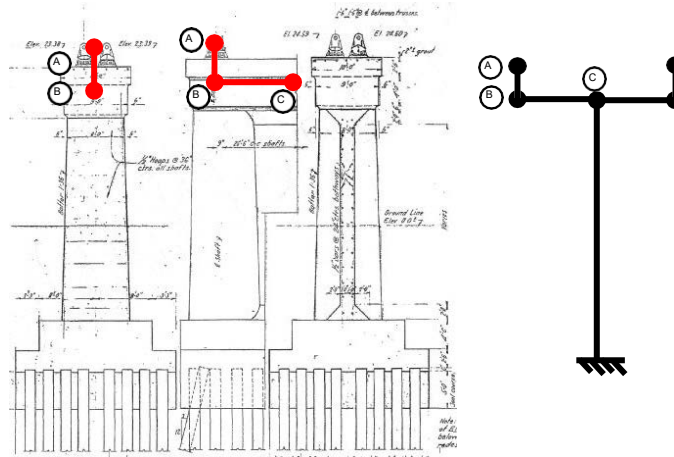


Figure 3.4 San Luis Ray Bridge As-Built Pier Layout

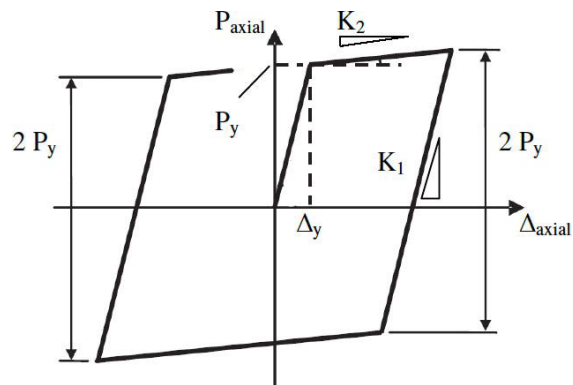


Figure 3.5 BRB Bilinear Model with Kinematic Hardening Rule

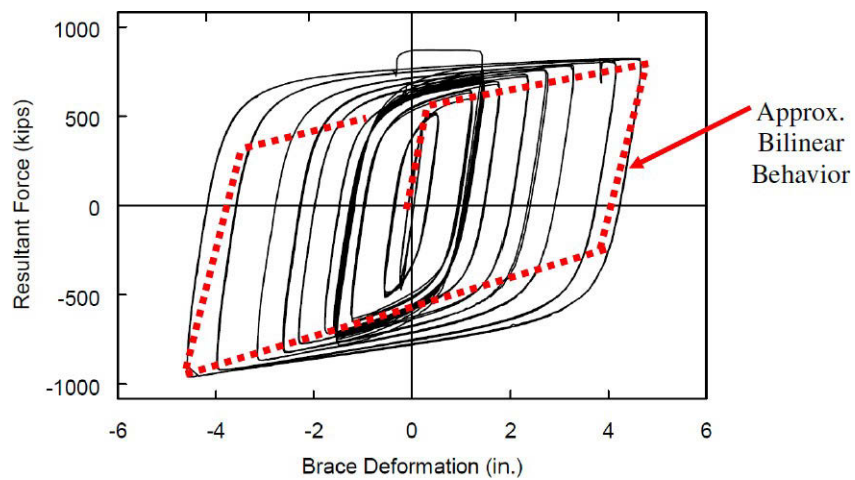


Figure 3.6 Typical BRB Hysteretic Behavior from Testing (Newell et al. 2003)

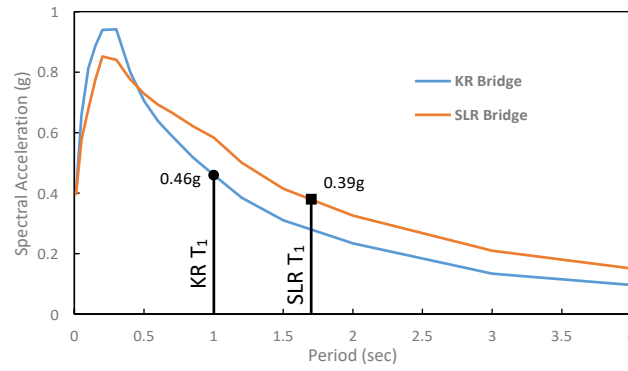


Figure 3.7 Design Response Spectra and Bridge Spectral Ordinates at the Fundamental Period

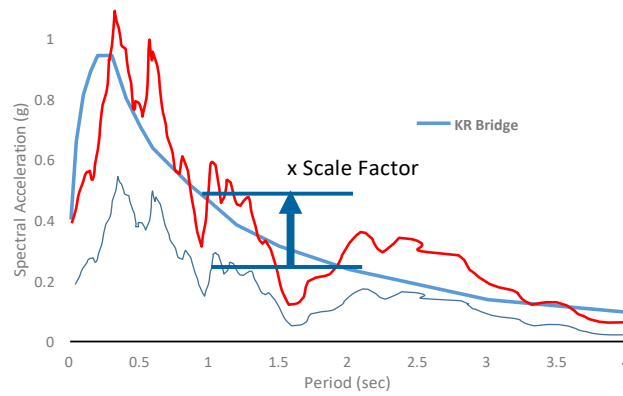
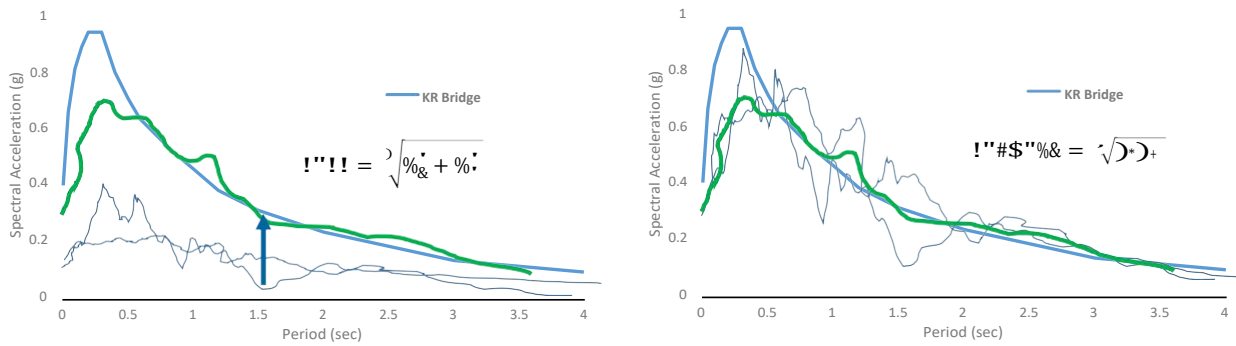


Figure 3.8 Ground Motion Suite Scaling Concept



(a) Two Horizontal Component Spectra Combined into a Representative Spectrum using the SSRS Method

(b) Two Horizontal Component Spectra Combined into a Representative Spectrum using the Geometric Mean Method

Figure 3.9 Spectra Combination Methods for Determining Ground Motion Scaling Factor

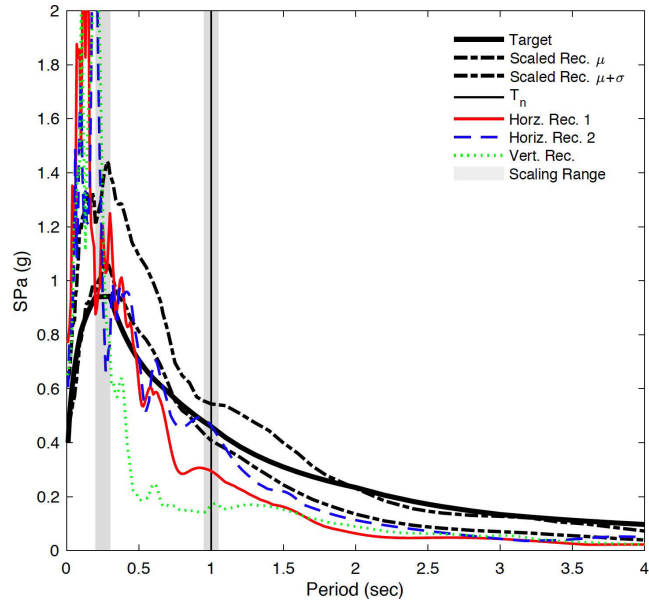


Figure 3.10 Klamath River Bridge Design Motion Spectra

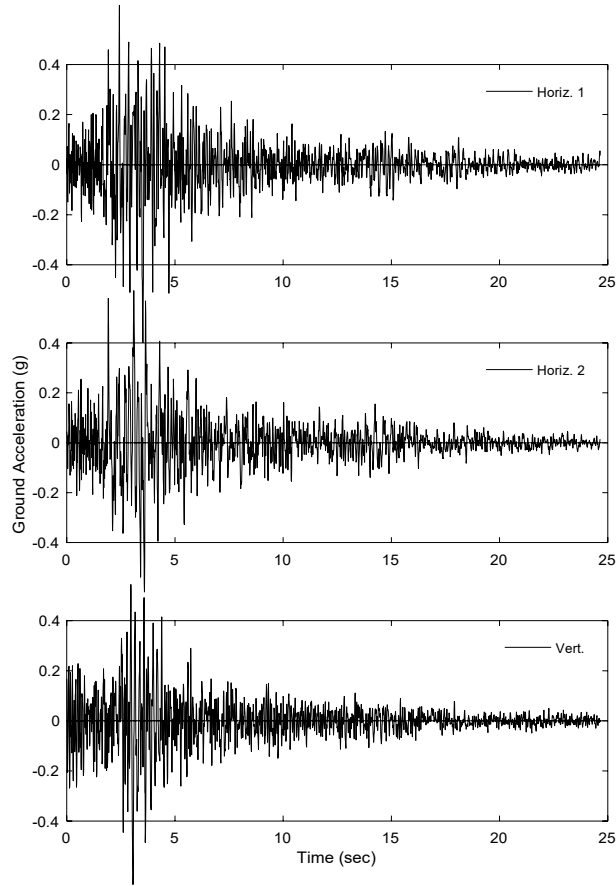


Figure 3.11 Klamath River Bridge Design Motion (See Table 3.3)

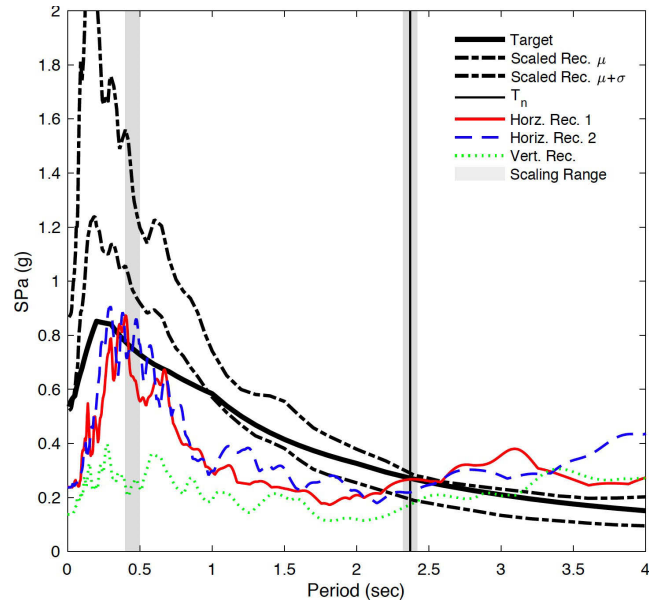


Figure 3.12 San Luis Ray River Bridge Design Motion Spectra

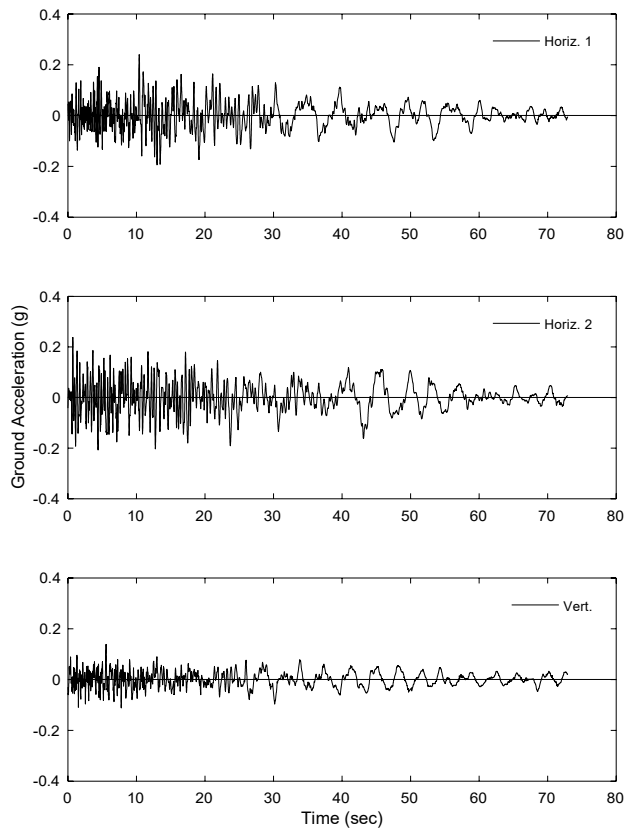


Figure 3.13 San Luis Ray River Bridge Design Motion (See Table 3.4)

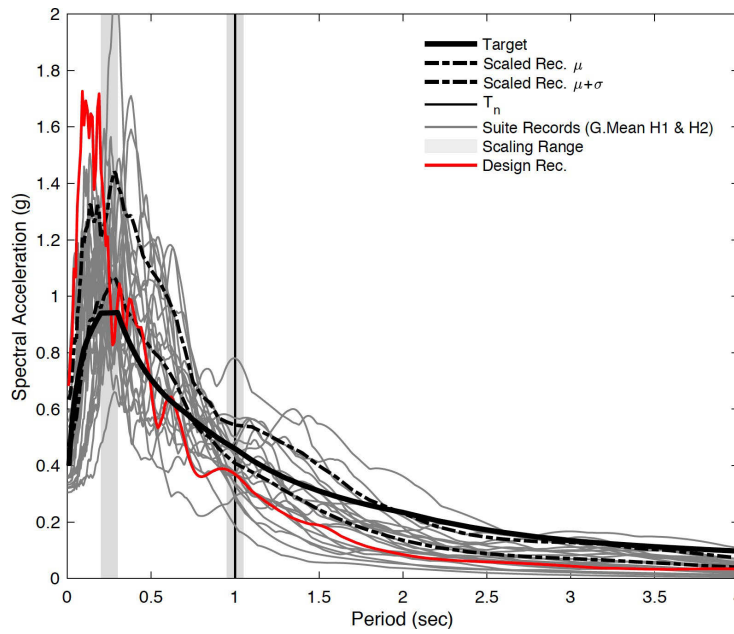


Figure 3.14 Klamath River Bridge Ground Motion Suite Spectral Summary

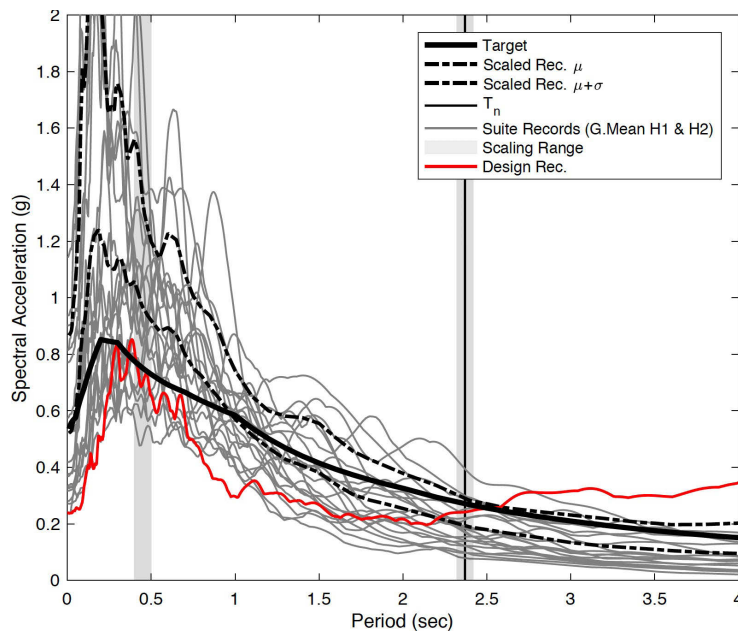


Figure 3.15 San Luis Ray River Bridge Ground Motion Suite Spectral Summary

4. BRIDGE BRB PARAMETRIC DESIGN

Due to the lack of an established BRB design procedure for bridge application, a parametric method was performed to identify the set of BRB characteristics which resulted in an improvement in bridge seismic performance. Here, the primary metric for improved performance was the decrease in failed original bridge truss members in the transverse trusses. Properties of the BRBs were varied incrementally in separate analyses using the design earthquake (See Sec. 3.2) to identify the approximately optimal BRB properties which minimized the number of failed elements in the model. Once BRB properties were found, the bridge model with BRBs was considered as the retrofitted bridge upon which the scaled suite of ground motions could be applied for development of the loading protocol (Sec 5). This chapter will briefly summarize the parametric design process and report the final BRB properties used for the subsequent suite analyses. Ultimately, the SLRB was not found to be an appropriate bridge candidate for BRB retrofit and thus the KRB was used for protocol development in Chapter 5.

4.1. Identification of BRB Locations

The initial step in designing BRBs for the bridges was to determine whether or not such ductile braces were even needed within the existing structures. Elastic time history analyses were conducted on the bridge models constructed from the as-built drawings with the design ground motions (Figure 3.10 through Figure 3.13). The maximum compressive forces of these original truss members were compared to their flexural buckling strengths, as given by Chapter E of AISC 360-10. Any members with a demand versus capacity ratio greater than unity was considered as failed, since this would indicate that a compressive failure occurred during the design earthquake. As shown in Table 4.1 through Table 4.3, in the Elastic Model column, both bridges experienced many instances of failed members. In the KRB, a concentration of failed members was observed around the bridge piers, evident in Figure 4.1. For SLRB, in Figure 4.2, many members exceeded their basic flexural buckling capacities in the group locations indicated. Most critical were those in Group 2 and 3, since they represent the primary transverse vertical frame at the end of the main truss spans. Both bridge behaviors indicated that the transverse trusses of the as-built bridges were in need of structural fuses to limit the force transmitted to the rest of the structure. This was attempted by replacement of strategic transverse truss members with BRBs.

This strategy followed the subsequent logic. The transverse direction of the bridge can be thought of as a continuous beam spanning between the abutments and the piers, which act as simple supports. The bridge represents a roughly uniformly distributed mass. When the deck mass experiences an acceleration, due to ground shaking, it can be reasonably assumed to result in an approximately uniform lateral force resisted by the lateral truss system. The resulting shear diagram would be at its maximum near the bridge piers and therefore these locations were good candidates for structural fuses. Hence, transverse truss elements were replaced by BRB elements in an attempt to relieve the structure of this excessive lateral shearing action. The BRB schemes are displayed in Figure 4.3 and Figure 4.4 for the KRB and SLRB, respectively.

4.2. BRB Parameterization

The following BRB parameter scheme was carried out on each bridge using, essentially, the same strategy. A bilinear BRB model was used (as described in Figure 3.5) with elastic stiffness given as

$$K = \frac{E A_{BRB}}{L_y} \quad (4-1)$$

where A_{BRB} is the BRB core area, L_y is the core yield length (See Figure 2.1), and E is the modulus of elasticity of steel (= 29,000 ksi). The bilinear element has only one post-yield slope which was assumed to be about 3% of the initial elastic stiffness. This value was based on other studies summarized by Lanning et al., 2011 (where the parameter was α), which also supported holding this value constant (i.e., no appreciable difference in structure response was observed with varying post-yield slope).

However, each BRB parameter in the previous equation, A_{BRB} and L_y , was varied in the parametric study. From Figure 2.1, the yielding length of the BRB is indicated. This is the portion of the BRB core which is smaller in cross section than the ends which serve as the brace connection points. These end segments are not intended to yield since they are not contained within the restraining steel tube and decoupled concrete mortar. Hence, all BRB yielding cores are shorter in length than the overall brace length. Here,

$$\beta = \frac{L_y}{L} \quad (4-2)$$

where L_{total} is the overall brace length from work point to work point, and β is the yielding core length parameterizing factor.

The area of the yielding steel core, A_{BRB} , was parameterized in a way which made it easy to relate the yielding force of the BRB to the original bridge truss members. The BRB yield force is

$$P_y = F_y A_{BRB} \quad (4-3)$$

where F_y is the yield stress of the BRB steel material, typically A36 ($F_y = 36$ ksi). The relationship between the BRB core area and the original truss members was taken as

$$A_{BRB} = \frac{P_{cr}}{R_y F_y \gamma} \quad (4-4)$$

where P_{cr} is the flexural buckling force of the original truss elements as defined by the AISC Manual of Steel Construction (ASCE 360-10), R_y ($= 1.5$ for rolled bars) is the ratio of the expected tensile strength to the nominal tensile strength (AISC 341-10) making the product of $R_y F_y$ equal to the expected yield stress of A36 steel ($= 54$ ksi), and γ is the core area parameterizing factor.

4.3. Parametric Analysis Results

Klamath River Bridge (KRB)

Here, a summarized version of the parametric results is presented for brevity. A number of different schemes were investigated and, as implied in the previous section, more parameter spaces were explored, many instances of which did not result in interesting bridge responses. For instance, varying the yield length on the KRB was determined to be of minimal influence on the overall bridge performance and resulting BRB demands. This is a departure from the previous study (Lanning et al. 2011) with BRB parametric study performed on the Vincent Thomas Bridge. For this bridge, the overall length of the BRBs was not variable due to one-to-one replacement of existing members being the only retrofit options considered. In the prior study, this was not the case. Therefore, for KRB this meant only very small changes in the yielding core area were possible. Although considerable effort was taken to make this trend clear in the analyses, it is not reported here for brevity.

The same can be said about the consideration of the yielding core length on the KRB, where a wider range of BRB core areas were explored. However, it was found that only a relatively

narrow range of core areas generated significant results. This, initially, indicated the fairly straightforward application of BRBs to steel truss bridges, which was first thought promising for future study into the direct BRB design approach. However, the scope of this study was to simply identify a beneficial BRB scheme and use it to obtain a general sense of the required cyclic response of BRB on this bridge type. Even a conservative design would be more desirable, for this work, than an exact BRB design.

As discussed in Section 4.1, the existing truss elements were replaced with BRBs in order to relieve the structures from a large number of buckled ($D/C > 1$) members. By varying the value of γ , the BRB core area was steadily decreased in relation to the original truss members flexural buckling strength. Table 4.1 shows the clear trend in decreasing the core area. For KRB, γ equal to 0.3 resulted in zero buckled members in the bridge. Further, the maximum drift at mid-span remained relatively unchanged, and actually decreased somewhat. Another indication of these BRB performing as desired is shown in Figure 4.5 where, when the value of γ decreases, the increased BRB hysteretic behavior (more loops) indicates more energy dissipation (as given by the area within the hysteresis loop). For instance, if the BRB does not yield or yields very little, then it is not acting as a structural fuse where the force imparted to the surrounding structure is limited by the yielding and subsequent very low axial stiffness during BRB yielding.

Therefore, the BRB retrofit design was selected as a core area corresponding to γ of 0.3. It should be noted that this is not proposed as an actual retrofit solution, rather the term retrofitted is used only to indicate that some original bridge truss elements were replaced with BRBs. This model was then subjected to the suite of ground motions described in Chapter 3, in order to generate the BRB loading protocol for braces applied to steel truss bridges, in Chapter 5.

San Luis Ray River Bridge (SLRB)

The BRB schemes and variables were studied extensively for the SLRB retrofit. Unfortunately, no combination in the very large parameter space yielded results that represented an improved bridge seismic performance, nor did almost any cases exhibit BRB yielding in nonlinear hysteretic loops. As displayed in Table 4.2 through Table 4.3, various elements were obviously originally designed to serve only as tension members so despite having a demand versus capacity ratio greater than one, they were not counted as failed members (i.e., these member can yield in tension without risk of member failure or any appreciable destabilizing effect on the bridge). Further, however, many truss members in the vertical lateral frames at the piers (Groups

2, 3, 5) were considered as failed during the design earthquake record. Hence, Group 2 was studied as the primary location of BRB for retrofit, as seen in Figure 4.4. Since the original frame was of a double-x configuration, which is not conducive to BRB implementation, a chevron style was investigated.

As in the KRB case, many more BRB parameter combinations were considered than are summarized in Table 4.3. The scheme (layout) of BRB in all these cases contained BRBs in Group 2 replaced by BRB at the pier locations. However, the last column of the table shows results from considering all Group 2 members as BRBs. From this table, it is evident that over a large parameter space containing variations in both β and γ , that no reduction of buckled members was attained. This was somewhat unsurprising upon inspection of the BRB cyclic behavior in these cases, because almost no BRB yielding could be observed.

Speculation as to the cause of this behavior included the drastic change in the frame transverse stiffness, and therefore a redistribution (even within the elastic-range) of forces away from the BRB locations. A comparison was made and summarized in Table 4.4. It was thought that perhaps BRB must be provided to retain the frame stiffness, and a γ value of between 1 and 2 is shown to provide just that. However, this was also found to result in no benefit.

Since no beneficial BRB scheme or parameter combination was able to be identified, the SLRB was not considered in the development of the protocol. Although this does not enrich the protocol data, it does shed light on the potential future study towards a BRB design procedure for steel truss bridges. This motivates the recommendation for future work related to the bridge BRB design process, in Section 6.3.

Table 4.1 Summary of Parametric Study for BRB Design, Klamath River Bridge

| Group No. | Section | Length (in) | F_{cr} (ksi) | No. Failed Members Demand/Capacity > 1 | | | |
|--|--------------|-------------|----------------|--|-------------------|------------|-------------|
| | | | | Elastic Model | Value of γ | | |
| | | | | | 0.9 | 0.6 | 0.3* |
| 1 | 6 WF 18 | 167 | 17.5 | 11 | 4 | 1 | - |
| 2 | 6 WF 18 | 164 | 17.9 | - | - | - | - |
| 3 | 6 WF 18 | 189 | 15.1 | - | - | - | - |
| 4 | 6 WF 18 | 96 | 25.1 | 2 | 2 | - | - |
| 5 | 6 WF 18 | 157 | 18.8 | - | - | - | - |
| 6 | 2LS 4x4x5/8 | 178 | 16.8 | 5 | 2 | - | - |
| 8 | 2LS 4x3x5/16 | 178 | 12.7 | 2 | - | - | - |
| 9 | 2LS 4x3x5/16 | 145 | 17.0 | - | - | - | - |
| 10 | 2LS 4x3x5/16 | 188 | 11.4 | 8 | 8 | 2 | - |
| 11 | 2LS 4x3x5/16 | 164 | 14.4 | - | - | - | - |
| 12 | 2LS 4x3x5/16 | 158 | 15.2 | - | - | - | - |
| Total | | | | 28 | 16 | 3 | 0 |
| Max Displacement Mid-Span (in.) | | | | 7.4 | 7.6 | 7.4 | 6.5 |

* Value selected for BRB properties in the retrofitted bridge design

Table 4.2 San Luis Ray Bridge Transverse Truss Member Properties

| Group No. | Section | Length (in) | F_{cr} (ksi) | KL/r_{min} | $4.71\sqrt{E/F_y}$ |
|----------------|-----------------------------|-------------|----------------|--------------|--------------------|
| 1 ^a | 2L 3.5x3x5/16 + PL 2.5x5/16 | 231 | 3.8 | 257 | 146 |
| 2 | 2L 5x3x5/16 | 137 | 16.1 | 119 | |
| 3 | 2L 5x3.5x5/16 | 168 | 15.6 | 122 | |
| 4 ^b | L 3.5x3x5/16 | 137 | 11 | 151 | |
| 5 | 2L 4x3x5/16 | 168 | 13.6 | 134 | |

^a Truss elements clearly designed as a tension member only

^b Truss elements likely designed as a tension member only

Table 4.3 Summary of Parametric Study for BRB Design, San Luis Ray Bridge

| Group No. | Elastic Model | No. Failed Members Demand/Capacity > 1 | | | | | | |
|---|------------------|--|--------------|--------------|--------------|--------------|--------------|----------------|
| | | β | | | | | | |
| | | 0.6 | | 0.5 | | 0.4 | | 0.4* |
| | | $\gamma=0.6$ | $\gamma=0.3$ | $\gamma=0.6$ | $\gamma=0.3$ | $\gamma=0.6$ | $\gamma=0.3$ | $\gamma=0.3^*$ |
| 1 ^a | 104 ^a | 109 | 109 | 108 | 108 | 108 | 106 | 100 |
| 2 | 52 | 32 | 32 | 32 | 32 | 32 | 32 | 0* |
| 3 | 8 | 22 | 18 | 22 | 18 | 18 | 16 | 16 |
| 4 ^b | 148 ^b | 96 | 98 | 94 | 97 | 82 | 95 | 98 |
| 5 | 22 | 16 | 16 | 16 | 16 | 16 | 16 | 16 |
| Total ($KL/r > 4.71\sqrt{E/F_y}$) | 82 | 70 | 66 | 70 | 66 | 66 | 64 | 32* |

^a Truss elements clearly designed as a tension member only

^b Truss elements likely designed as a tension member only

* All Group 2 members replaced with BRB

Table 4.4 Representative Transverse Truss End Frame Stiffnesses, San Luis Ray Bridge

| BRB Parameters | γY | βY | P_y (kips) | Δ_y (in.) | Frame Transverse Stiffness, K (kips/in) |
|-----------------|------------|-----------|--------------|------------------|---|
| BRB Frame Cases | 0.3 | 0.75 | 22.7 | 0.318 | 33 |
| | 0.3 | 0.6 | 22.7 | 0.25 | 40 |
| | 0.3 | 0.5 | 22.7 | 0.21 | 48 |
| | 0.3 | 0.4 | 22.7 | 0.17 | 58 |
| | 1 | 0.5 | 75 | 0.21 | 217 |
| | 2 | 0.5 | 151 | 0.21 | 346 |
| Frame | - | - | - | - | 313 |

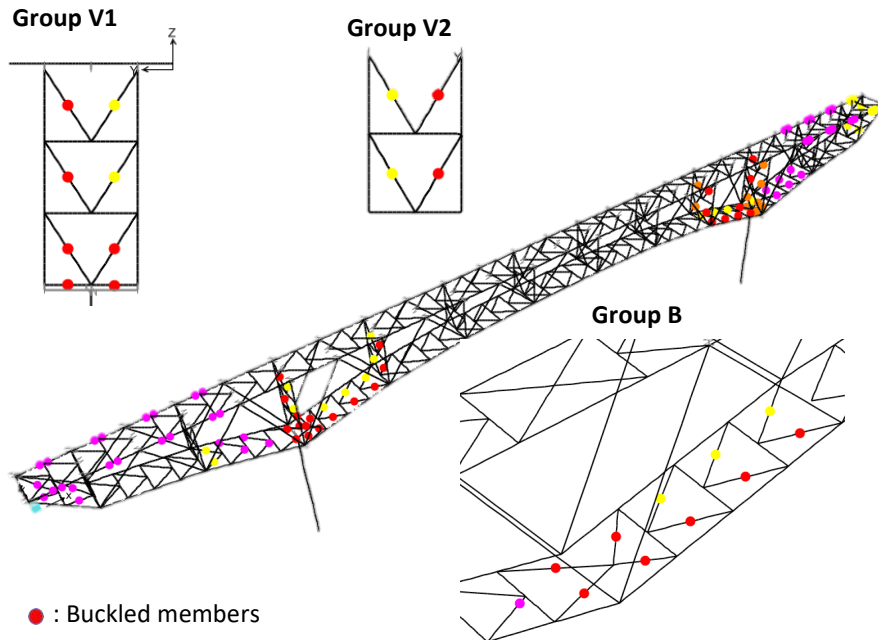


Figure 4.1 Original Truss Member Failing under Design Motion, Klamath River Bridge

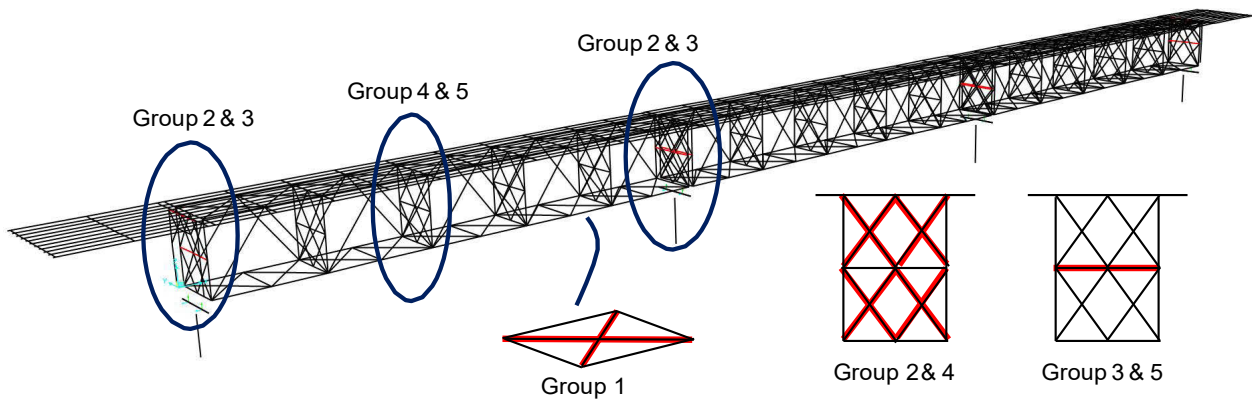


Figure 4.2 Original Truss Member Buckling under Design Motion, San Luis Ray River Bridge

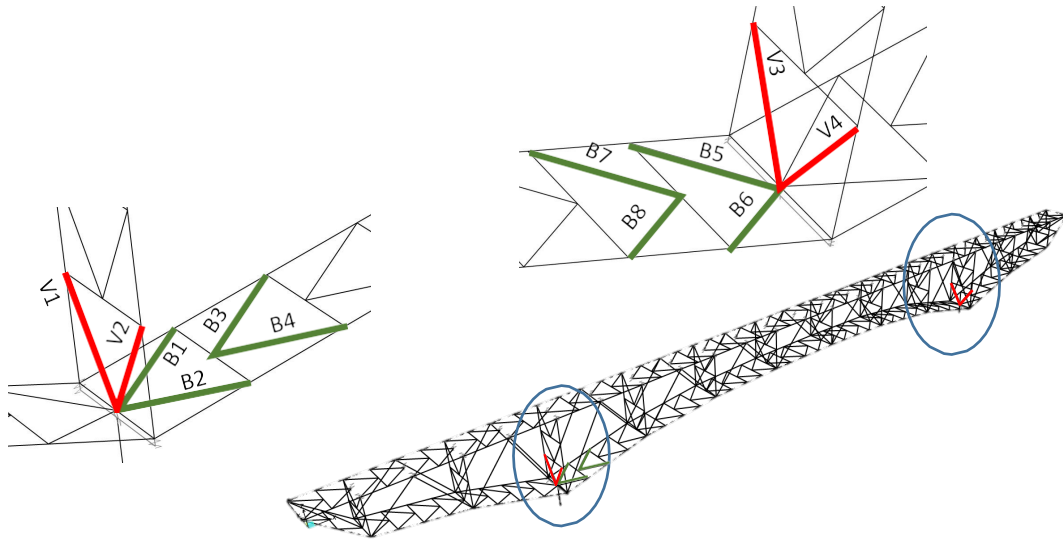


Figure 4.3 Location of BRB, Klamath River Bridge

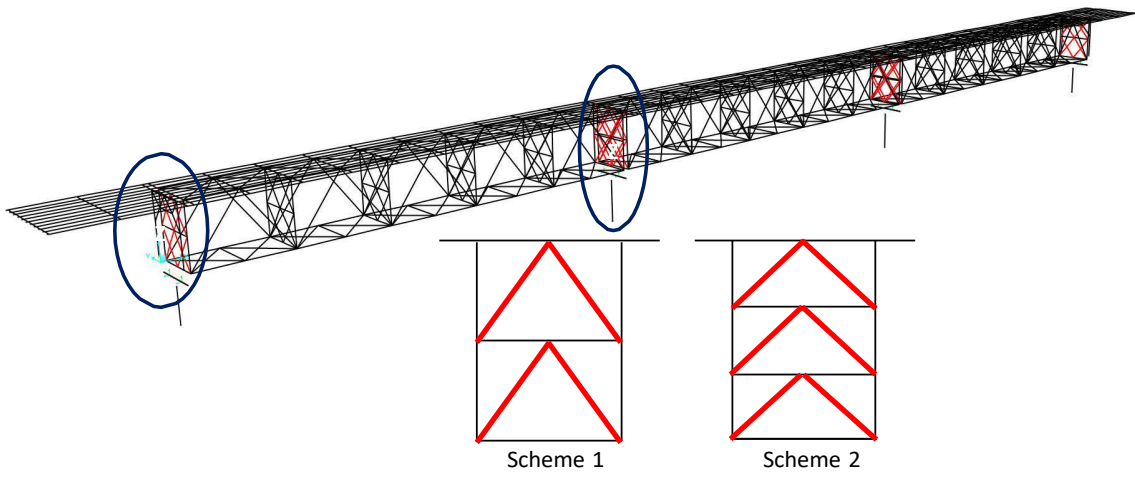
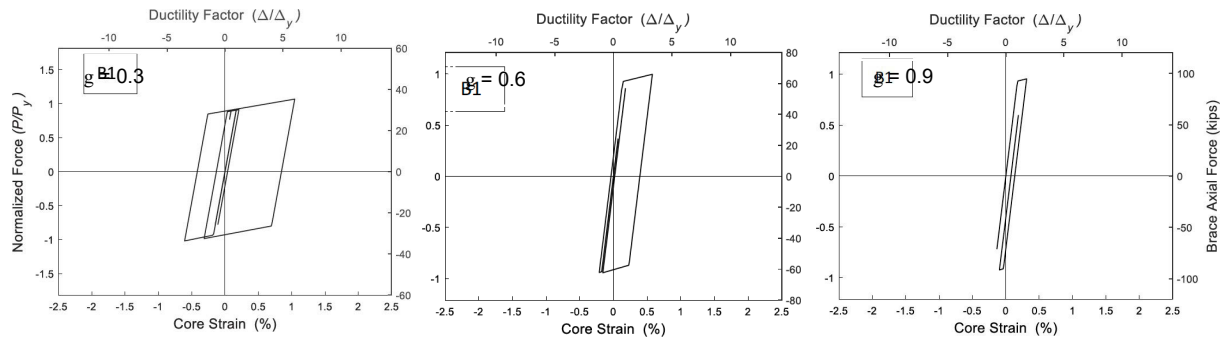
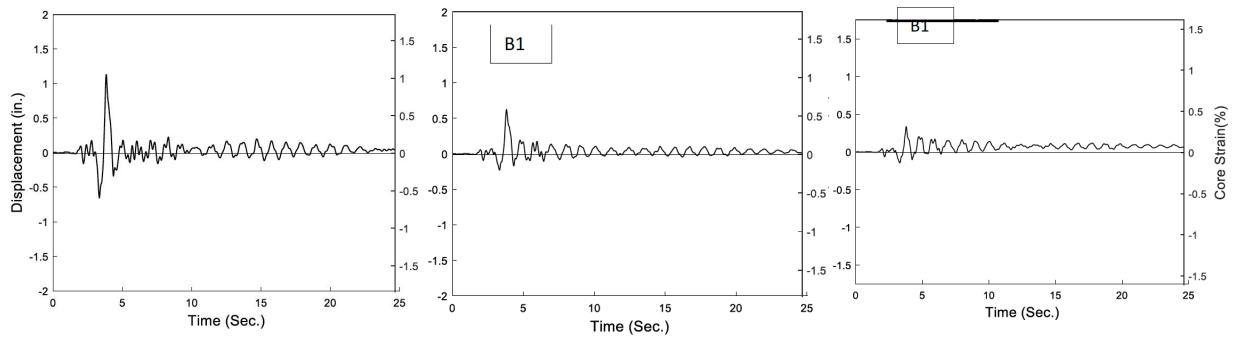


Figure 4.4 Location of BRB, San Luis Ray River Bridge



(a) Brace Hysteretic Response



(b) Brace Deformation Time History

Figure 4.5 Example KRB BRB Response under Design Ground Motion, Varied γ Value

5. PROTOCOL DEVELOPMENT

5.1. Protocol Characteristics

With a BRB retrofit design for each bridge identified, the ground motion suite described in Section 3.2 was applied to the KRB. The resulting BRB cyclic responses were collected and carefully inspected for trends. One primary observation was that very little BRB inelastic residual deformation was evident in almost all ground motion results. This indicates that BRB cycles remained mostly symmetric about zero deformation, which simplifies the development of a representative loading protocol as it need not explicitly reflect a residual deformation. Therefore, the basic cycle counting does not need to consider “where” cycles occurred relative to zero because cycles are generally centered around zero net deformation. A few examples of the brace deformation time histories are shown in Figure 5.1 in the left columns. Generally, the cycles are centered about zero, and note the variation provided by the different ground motions in the suite.

Cycle counting was performed using the Rainflow cycle counting process (ASTM E 1049) which decomposes complex cyclic time histories into a count of various amplitude excursions (one cycle is formed of two excursions). From the excursion count, the excursions within the elastic range can be eliminated, leaving only the damaging inelastic excursions. In the right column of Figure 5.1, the Rainflow excursion count is shown for these few examples. The first histogram column was ignored in the formation of the protocol because this indicates an excursion only equal to the yield deformation (i.e., no yielding occurred in these excursions). Again, the variation provided by the suite is apparent.

From the excursion counting algorithm it was possible to obtain the mean and standard deviation of the number of excursions within each increment of yield deformation. Therefore, the protocol could be made to reflect the number of excursions at each amplitude. The results of this statistical summary are shown in Figure 5.2 for KRB. Brace B5 was deemed as the representative case since it contained the most severe cycle count, the largest absolute maximum BRB deformation, shown in Table 5.1, and the largest cumulative ductility, shown in Figure 5.4.

These characteristics were all considered when forming the KRB Protocol shown in Figure 5.5. Excursions were centered around zero deformation, alternated in tension and compression directions (arbitrarily started in compression) and incrementally increased to the maximum deformation value following, in general, the Rainflow excursion count histogram progression.

Once maximum deformation was attained, the excursions were returned to the last statistically significant amplitude value and repeated, in an alternating fashion so as to create cycles, until the cumulative ductility value (= 200) was obtained to match the suite statistics.

5.2. Protocol Analysis

The KRB Protocol is compared to the AISC BRB Protocol of AISC 341-10 in Figure 5.6. There are similarities, for instance (as shown in Figure 5.4) the 84th-percentile KRB Protocol cumulative ductility value approaches 200. This is consistent with the AISC Protocol; however, it is evident that the amplitudes of the AISC Protocol are larger than those of the KRB. This results in the AISC Protocol applying the inelastic damage more aggressively, as Figure 5.7 shows. Further, many BRB testing studies (Merritt et al., 2003, Newall et al., 2005, Lanning et al., 2011, among others) have shown that BRBs easily sustain larger amplitudes and many more inelastic cycles than either the AISC or KRB Protocols contain. Therefore, the slightly larger number of cycles within the KRB Protocol is insignificant. Hence, the AISC Protocol is more severe than the KRB. The implications of this are discussed in below in Section 6.2.

Table 5.1 Absolute Maximum BRB Deformation Statistics, Klamath River Bridge Suite

| | Max Δ_y | Min Δ_y |
|-----------------|----------------|----------------|
| Average | 6.2 | -5.40 |
| STDV | 2.7 | -2.25 |
| Avg+STDV | 8.8 | -7.65 |

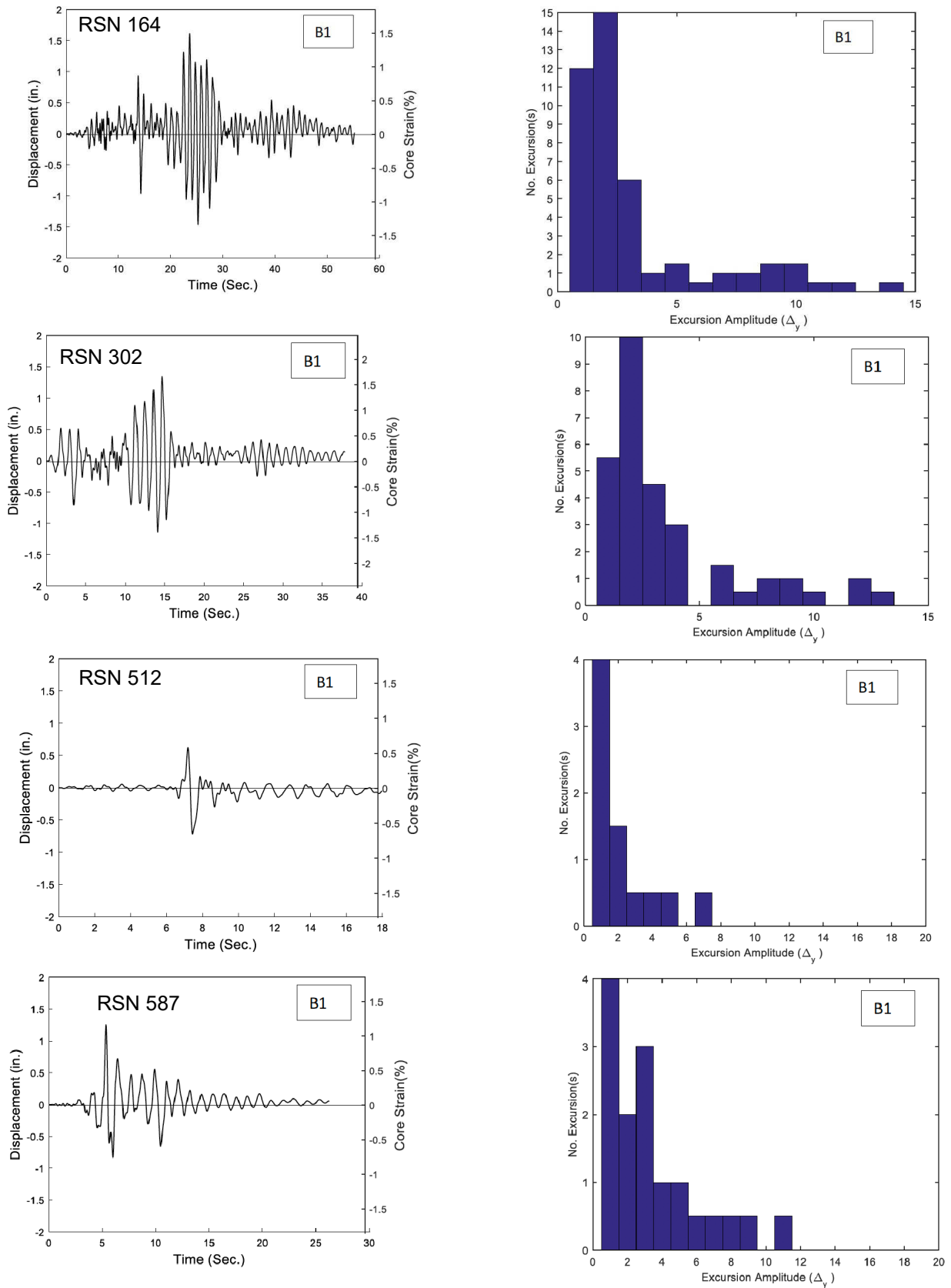


Figure 5.1 Examples of BRB Responses from KRB Ground Motion Suite

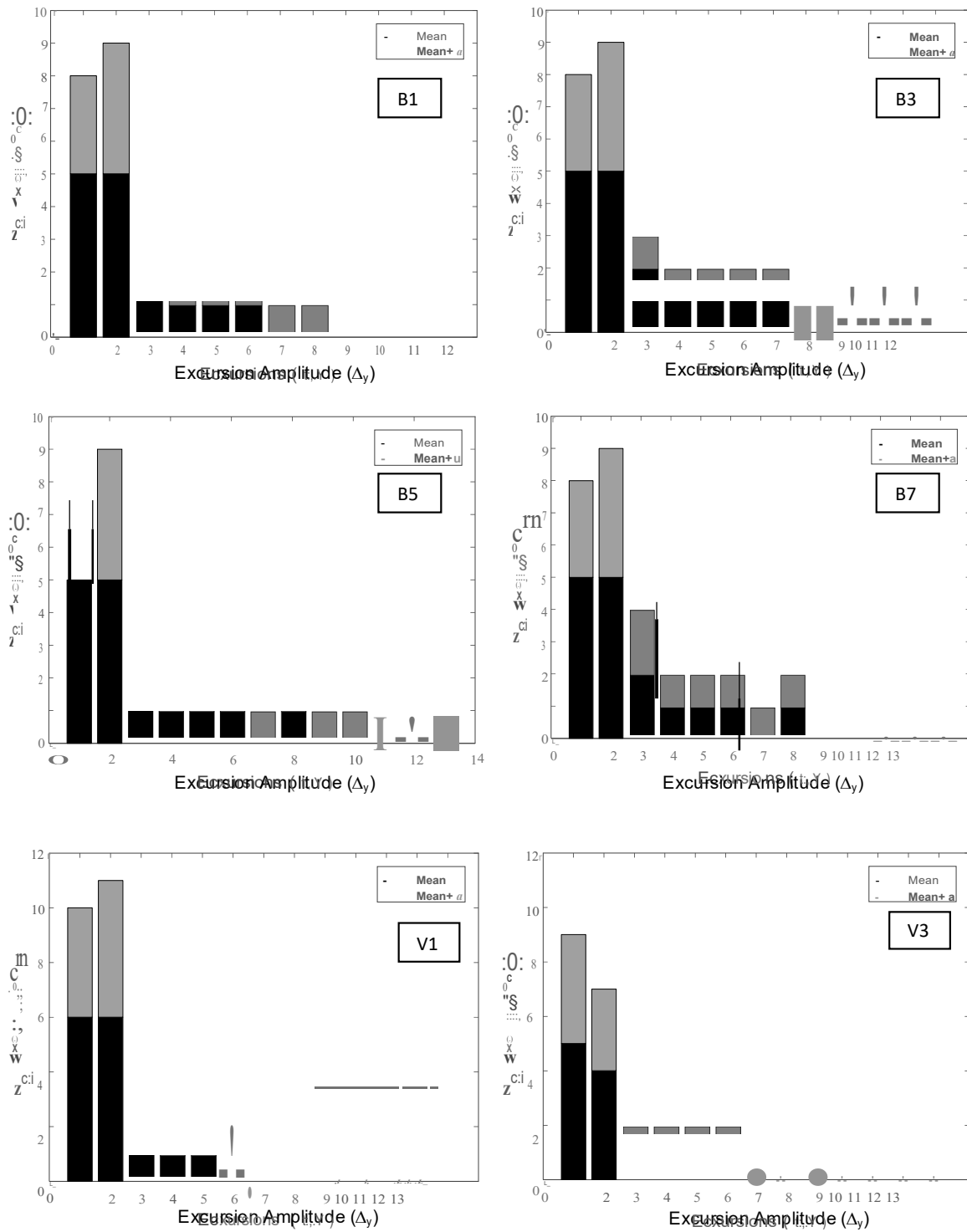


Figure 5.2 KRB Suite BRB Statistical Summary of Rainflow Excursion Counting

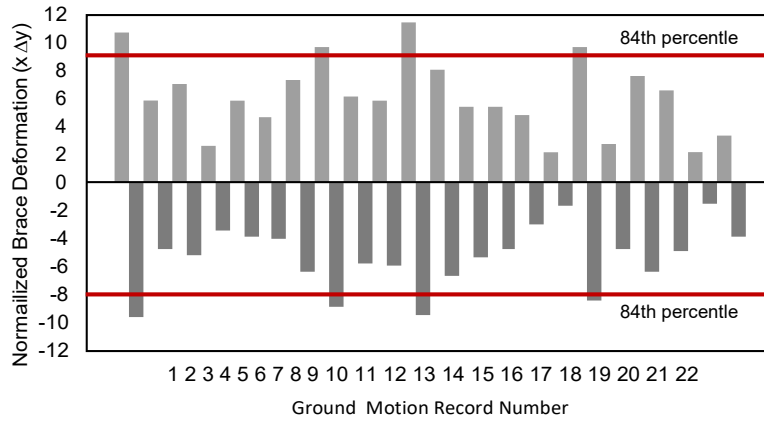


Figure 5.3 KRB Loading Protocol for BRB

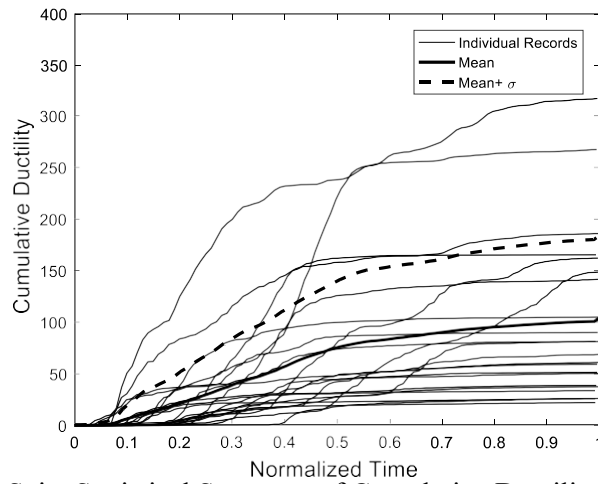


Figure 5.4 KRB Suite Statistical Summary of Cumulative Ductility, BRB B5 Location

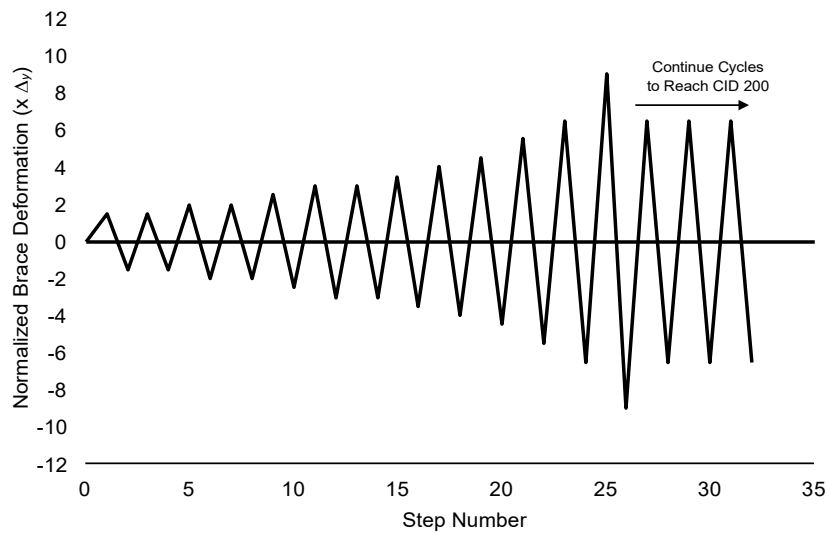


Figure 5.5 KRB Loading Protocol for BRB

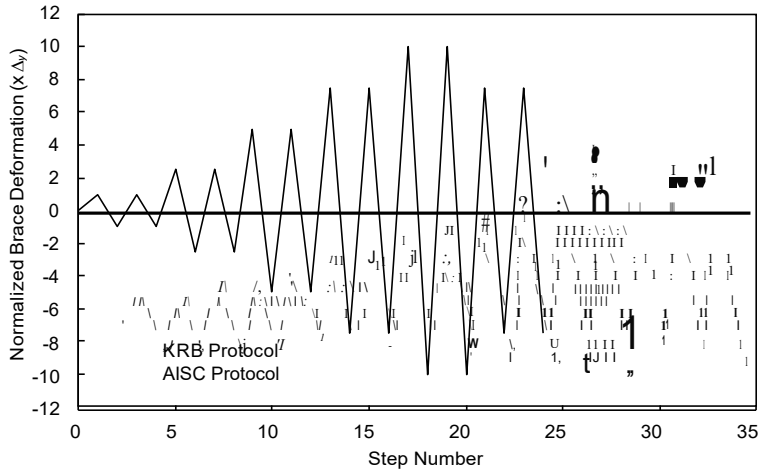


Figure 5.6 Comparison of KRB and AISC BRB Protocols

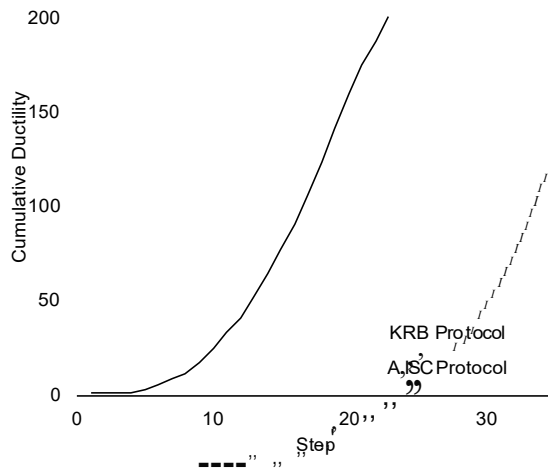


Figure 5.7 Comparison of the Cumulative Ductility Distribution of KRB and AISC BRB Protocols

6. SUMMARY AND RECOMMENDATIONS

6.1. Summary of Analyses and Results

Two existing steel truss bridges were modeled and subjected to ground motions considered as design-level to contemporary standards. Both bridges were observed to sustain fairly heavy damage under this shaking in the form of many failed transverse truss members. In this elastic analysis, truss members whose demand versus capacity ratio was larger than unity was considered as buckled and therefore failed. Truss members at strategic locations along the bridge, many coinciding with failed members, were replaced with BRBs modeled with inelastic truss elements following a bilinear cyclic rule with kinematic hardening. The BRB yielding core area was then varied to determine the approximately optimum value, indicated by the reduction of the number of buckled members bridge-wide. Only BRBs for the Klamath River Bridge were successfully identified, despite a large parameter space being considered for the San Luis Ray Bridge.

The KRB model, retrofitted with the proper BRBs, was then subjected to a suite of over 20 scaled ground motions. The resulting BRB cyclic responses were collected and analyzed. Brace cyclic response metrics of maximum brace deformation, inelastic excursion count, and total cumulative ductility were recorded, and they informed the formation of a representative BRB loading protocol, the KRB Protocol (Figure 5.5). This protocol reflects the 84th-percentile (mean plus one standard deviation) of the BRB demands from the suites applied to the steel truss bridge.

The KRB Protocol exhibits inelastic cyclic characteristics similar to those of the AISC protocol for BRBs within building frames. The overall accumulated ductility (~200) and general pattern of cyclic amplitude (See Figure 5.6) are very similar, however overall the maximum brace deformation amplitudes of the AISC protocol are larger. The distribution of cumulative ductility is directly indicative of the inelastic damage inflicted on the braces during the prequalifying test. As is evident in Figure 5.7, the AISC protocol is more severe.

6.2. Protocol Recommendations

Given the similarities of the two protocols and the prior wide-spread use of the AISC protocol in prequalify many existing BRB component designs, the KRB Protocol developed here is not suggested for enforcement on BRBs to be used on steel truss bridges. Rather, the AISC protocol seems sufficient and conservative for this purpose, although this study only confirms that

assertion for the KRB itself. This means that BRBs passing the AISC Protocol have been proven to possess inelastic capabilities beyond that required by a BRB within a steel truss bridge structure significantly similar to the KRB.

This is beneficial for bridge designers because existing BRB designs having already been prequalified under the AISC standard may therefore be immediately considered for implementation on this type of steel truss bridge. This recommendation also considers the fact that many BRB tests have been conducted using the AISC protocol as a minimum achievement after which braces have been subjected to far more severe inelastic demands (Merritt et al., 2003, Newel et al., 2005, Lanning et al., 2012).

The AISC Protocol is defined in Chapter K of the AISC 2010, which requires the following loading sequence (depicted in Figure 2.4) to be applied to the test specimen:

- 1) 2 cycles of loading at the deformation corresponding to $\Delta_b = 1.0 \Delta_{by}$
- 2) 2 cycles of loading at the deformation corresponding to $\Delta_b = 0.5 \Delta_{bm}$
- 3) 2 cycles of loading at the deformation corresponding to $\Delta_b = 1.0 \Delta_{bm}$
- 4) 2 cycles of loading at the deformation corresponding to $\Delta_b = 1.5 \Delta_{bm}$
- 5) 2 cycles of loading at the deformation corresponding to $\Delta_b = 2.0 \Delta_{bm}$
- 6) Additional complete cycles of loading at the deformation corresponding to $\Delta_b = 1.5 \Delta_{bm}$ as required for the brace test specimen to achieve a cumulative inelastic axial deformation of at least 200 times the yield deformation (i.e., CID = 200).

where the deformation Δ_b is the steel core axial deformation of the test specimen. Note that Δ_{by} corresponds to the axial deformation at first significant yield, and Δ_{bm} is the axial deformation which corresponds to the design story drift of the building structure. The Δ_{bm} used in the AISC Protocol compared here, corresponds to the maximum 2%

Since the design drift of this (historic) bridge in this study is not available, nor can it be determined with much certainty, a direct comparison in terms of structure design drift is not made between the AISC Protocol and the KRB Protocol. However, since the bridge exhibited large amounts of failed transverse truss members under the design earthquake (of contemporary design intensity) it can be reasonably assumed that the design drift is much less than that experienced. Therefore, the BRB deformation demands experienced in the suites can also be reasonably assumed to be on the order of that required in the AISC protocol used in the comparisons shown in Figure 5.6 and Figure 5.7. In other words, with a steel truss bridge, significantly similar to the

KRB, design drift identified the AISC protocol values can be directly calculated using the scheme provided above.

In applying BRBs to truss bridges not significantly similar to the KRB, a suite of ground motions should be scaled to the appropriate design spectrum in order to carry out the protocol development procedure described in Chapter 5. By collecting and analyzing the BRB demand results, one can determine whether the specific bridge case will present statistically larger demands than that posed by the AISC Protocol, in which case a different bridge-specific protocol can be developed and used. However, this process represents an unreasonable amount of effort, data collection, and data analysis for the bridge design engineer considering the use of BRB.

There seem to be many similarities between steel truss bridge pier framing and building braced frames. These include brace configuration (e.g., chevron), frame dimensions and resulting brace lengths, and the small magnitudes of acceptable frame drift resulting in relatively small brace deformation. With these similarities in mind, together with the protocol comparison data point from this study, it is now more reasonable for a designer to consider the AISC Protocol to be sufficient for most steel truss bridge BRB applications. Before this study there was no such data point. The designer faced with deciding if an AISC-prequalified BRB is adequate for a particular bridge can consider the following to aid in their engineering judgement:

- 1) The BRB can be sized using a parametric method (a semi-optimized design solution) as is summarized in this study and by Lanning et al., 2011.
- 2) If the maximum BRB core axial deformation (either in tension or compression) is less than $5\Delta_y$, the AISC Protocol is most likely a very reasonable BRB performance metric. Therefore, an AISC-prequalified brace could reasonably be directly used for the application.
- 3) If the maximum BRB core axial deformation (either in tension or compression) is greater than $5\Delta_y$ but less than $10\Delta_y$, the AISC Protocol is most likely a reasonable BRB performance metric. However, the maximum protocol deformation could reasonably be increased to $15\Delta_y$, rather than the standard $10\Delta_y$ typically used in manufacturer BRB prequalification testing (Merritt et al., 2003, Newall et al., 2005, Lanning et al., 2012). It is likely, still, that manufacturers would have pre-existing test data to verify that their BRBs are fully capable of sustaining this hypothetical version of the AISC Protocol. Many BRB prequalifying tests are followed by additional larger cycles which often

approach or exceed these deformation levels. Hence, it may still be possible to directly use a BRB without additional prequalification testing.

- 4) If the maximum BRB core axial deformation (either in tension or compression) is greater than $10\Delta_y$, the AISC Protocol may not be satisfactory. The designer could specify that an AISC-prequalified BRB be subjected to a more strenuous AISC-style protocol with the maximum deformation value equal to 2 times the maximum observed from the design earthquake simulation.

The basis for these recommendations, specifically the factor of 2 applied to the maximum deformation, is taken from the AISC Protocol convention of requiring brace deformation resulting from 2 times the design story drift. This may be conservative, but with only one design motion considered in the above scenario it may not be overly conservative. It should be noted, though, that this is simply a recommendation based on the experience of the author in this and other BRB protocol studies. Without a properly developed prequalifying protocol, designers are forced to make decisions based on engineering judgment.

6.3. Recommendations for Future Work

(1) A more robust study should be conducted to properly advance the adoption of BRB into the bridge design industry and provide design engineers the tools needed to properly and efficiently utilize BRB on bridges. Archetypes of bridges, one being steel truss bridges, which are equipped with BRBs must be used to develop appropriate conclusions about the necessary prequalifying criteria. There are several features to be included in this larger study. (i) The site conditions and (ii) seismic hazards should be included in the ground motion variations. Further, (iii) additional directions/actions of BRB deformation (e.g., non-axial, or out-of-plane motions) must be considered in order to account for potential connection stresses particular to bridges. Without this additional information incorporated into the protocols, engineers are forced to either assume a loading protocol or use that provided by AISC. The current study provides an insight into the validity of assuming the AISC Protocol, however this result is not widely applicable.

Finally, (2) a proper BRB design procedure should be developed so as to further reduce the burden on the design engineer. Although it is reasonable for designers to conduct a parametric study for sizing the BRB to a particular bridge, a design procedure would provide confidence and

consistency throughout the industry. This procedure would need to be developed in coordination with AASHTO and Caltrans seismic design methodologies. Thus far, the difficulty arises from the fact that these standards often utilize a displacement-based philosophy rather than an equivalent lateral force method (like buildings using AISC and ASCE 7). Differences between new construction and retrofit BRB uses should be considered.

These two future objectives are interdependent as development of protocols requires proper design of BRB on bridges. Yet, case-by-case optimization, as performed in this study for KRB, would provide data to develop the design procedure.

REFERENCES

- AASHTO. (2017) AASHTO LRFD Bridge Design Specifications, American Association of State Highway and Transportation Officials, Washington, D.C.
- AISC 341-16. (2016). *Seismic provisions for structural steel buildings*, American Institute of Steel Construction, Chicago, IL.
- AISC 360-16. (2016). *Specifications for Structural Steel Buildings*, American Institute of Steel Construction, Chicago, IL.
- Caltrans (2016). *Seismic Design Specifications for Steel Bridges – 2nd Edition*. California Department of Transportation, Caltrans SDS, Sacramento, CA.
- Carden, L., Itani, A., Buckle, I., Aiken, I. (2004). “Buckling restrained braces for ductile end cross frames in steel plate girder bridges” *13th World Conf. on Earthquake Engineering*, Vancouver, Paper No. 503.
- Celik, O.C. and Bruneau, M. (2009). “Seismic behavior of bidirectional-resistant ductile end diaphragms with buckling restrained braces in straight steel bridges,” *Engineering Structures*, Vol. 31, pp. 380–393.
- CSi. (2016) *Computers & Structures, Inc., Bridge*. Computers & Structures, Inc., Walnut Creek, Calif.
- Di Sarno, L., Chiodi, R., Manfredi, G. (2013). “Seismic response analysis of existing non-ductile buildings retrofitted with BRBs” *Proc.*, 4th ECCOMAS Thematic Conference on Computational Methods in Struct. Dynamics and Earthq. Eng. Kos Island, Greece.
- Ge, H.B., Luo, X.Q., and Usami, T. (2008). “Damage control design of bridge in Japan,” *Proc.*, Tenth International Symposium on Structural Engineering for Young Experts, Changsha, China
- Kanaji, H., Fujino, Y., Watanabe, E., Suzuki, N. (2006). “Seismic retrofit of a long-span truss bridge applying damage control strategy,” *Proc.*, International Association for Bridge and Structural Engineering Conference, Copenhagen, Denmark.
- Kim, D.W., Sim, H.B., and Uang, C.M., and Uang, C.M. (2009). “Subassemblage testing of CoreBrace buckling-restrained braces (H series),” *Report No. TR-09/01*, Department of Structural Engineering, University of California, San Diego, La Jolla, CA.
- Krawinkler, H. (1983). “Recommendations for experimental studies on the seismic behavior of steel components and materials.” *John A. Blume Center Report No. 61*. Dept. of Civil Engineering, Stanford Univ., Stanford, Calif.
- Krawinkler, H. (1992). “Guidelines for cyclic seismic testing of components of steel structures” *ATC-24*, Applied Technology Council, Redwood City, Calif.
- Krawinkler, H. (2009). “Loading histories for cyclic tests in support of performance assessment of structural components” *3rd Internl. Conf. on Adv. in Experimental Struct. Engineering*, San Francisco.

- Lanning, J., Benzoni, G., Uang, C.M. (2011) "The feasibility of using buckling-restrained braces on long-span bridges: A case study" *Report No. SSRP-11/09*. Dept. of Structural Engineering, Univ. of California, San Diego, La Jolla, Calif.
- Lanning, J., Uang, C.M., Benzoni, G., (2012) "Subassemblage testing of CoreBrace buckling-restrained braces (P Series)" Testing Report Nos. *TR-12/03, TR-12/04, and TR-12/06*. Dept. of Structural Engineering, Univ. of California, San Diego, La Jolla, Calif.
- Lanning, J., Benzoni, G., Uang, C.M., (2013). "The feasibility of using buckling-restrained braces for long-span bridges: Near-fault loading protocols and full-scale testing." *Report No. SSRP 13/17*. Dept. of Structural Engineering, Univ. of California, San Diego, La Jolla, Calif.
- Lanning, J., Uang, C.M., (2014). "Testing and modeling of A36 and stainless steel buckling-restrained braces under near-fault loading conditions" *Proc., 5th Asia Conf. on Earthquake Eng.*, Oct. 2014, Taipei, Taiwan.
- Merritt, S., Uang, C.M., Benzoni, G., (2003). "Subassemblage testing of Star Seismic buckling-restrained braces" Testing Report No. *TR-03/04*. Dept. of Structural Engineering, Univ. of California, San Diego, La Jolla, Calif.
- Newell, J., Uang, C.M., and Benzoni, G. (2005). "Subassemblage testing of CoreBrace buckling-restrained braces (F series)," *Report No. TR-05/01*, Department of Structural Engineering, University of California, San Diego, La Jolla, CA.
- NIST. (2011). "Selecting and scaling earthquake ground motions for performing response-history analyses", *NIST GCR 11-917-15*, NEHRP Consultants Joint Venture, produced by the Applied Technology Council and the Consortium of Universities for Research in Earthquake Engineering for the National Institute of Standards and Technology, Gaithersburg, MD.
- PEER, Pacific Earthquake Engineering Research Center, PEER Ground Motion Database.
< <https://ngawest2.berkeley.edu/>>
- Reno, M. L., & Pohll, M. N. (2010). Seismic Retrofit of California's Auburn-Forest Hill Bridge. *Transportation Research Record: J. Transportation Research Board*, 2201(1), 83-94.
- Sabelli, R., Mahin, S., Chang, C., (2003). "Seismic demands on steel braced frame buildings with buckling-restrained braces" *Engineering Structures* 25(5), 655-666.
- Uang, C.M., Nakashima, M., and Tsai, K.C., (2004). "Research and application of buckling-restrained braced frames," *International J. of Steel Structures*, 4(4), 301-313.
- Usami, T., Lu, Z., Ge, H. (2005) "A seismic upgrading method for steel arch bridges using buckling-restrained braces" *Earthquake Engng Struct. Dyn.*, 34, 471-496
- Wada, A., Huang, Y. and Bertero, V.V. (2004). "Innovative strategies in earthquake engineering," Chapter 10 in *Earthquake engineering: from engineering seismology to performance-based engineering*, edited by Bozorgnia, Y. and Bertero, V.V., CRC Press.
- Xie, Q. (2005). "State of the art of buckling-restrained braces in Asia," *J. of Constructional Steel Research*, Vol. 61, pp. 727-748.

APPENDIX

The ground motions used for protocol development, listed in Table 3.3 and Table 3.4, are provided here for reference.

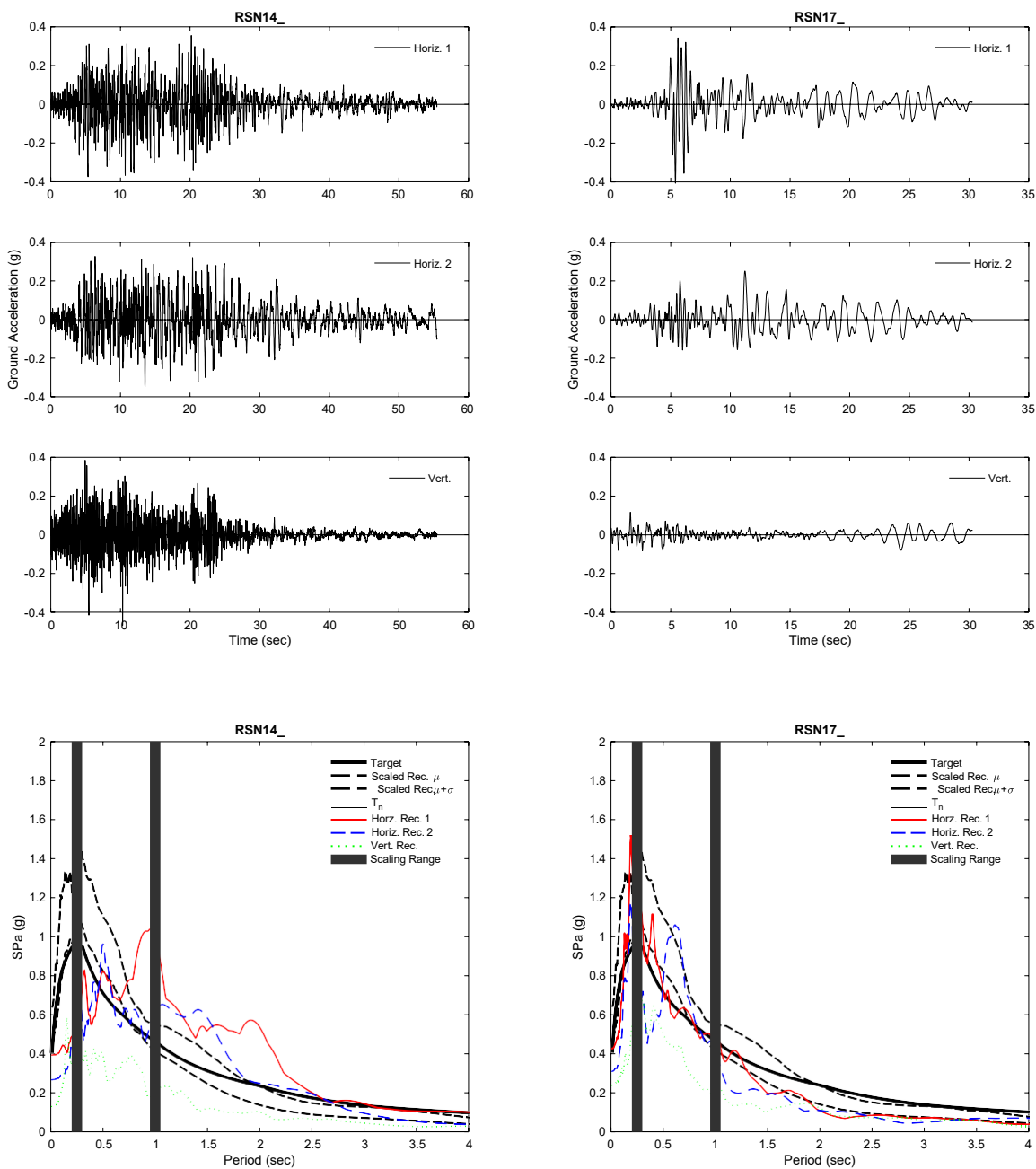


Figure A.1 Klamath River Bridge Ground Motion Suite Time Histories and Spectra

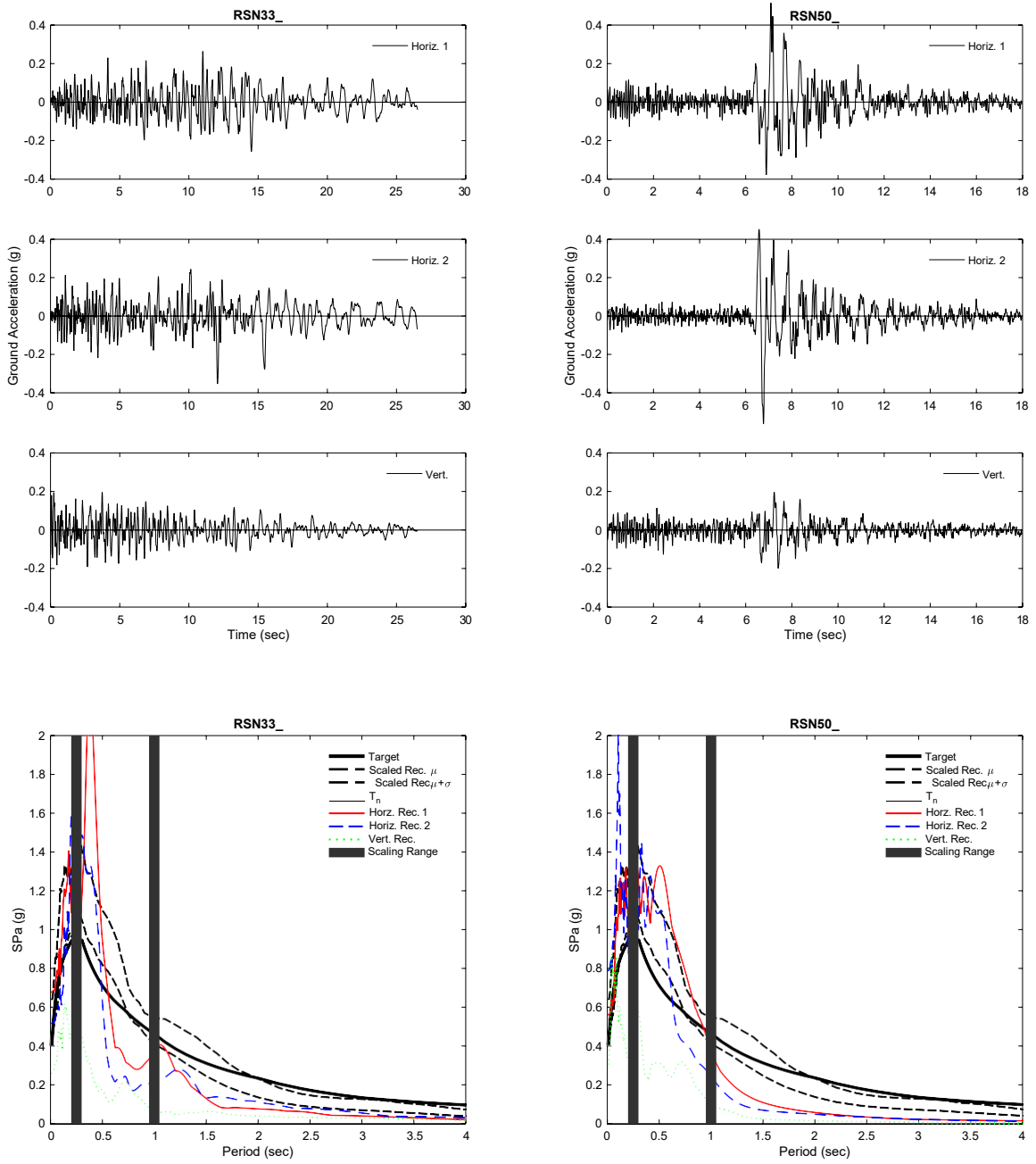


Figure A.1 Klamath River Bridge Ground Motion Scaled Suite Time Histories and Spectra (Continued)

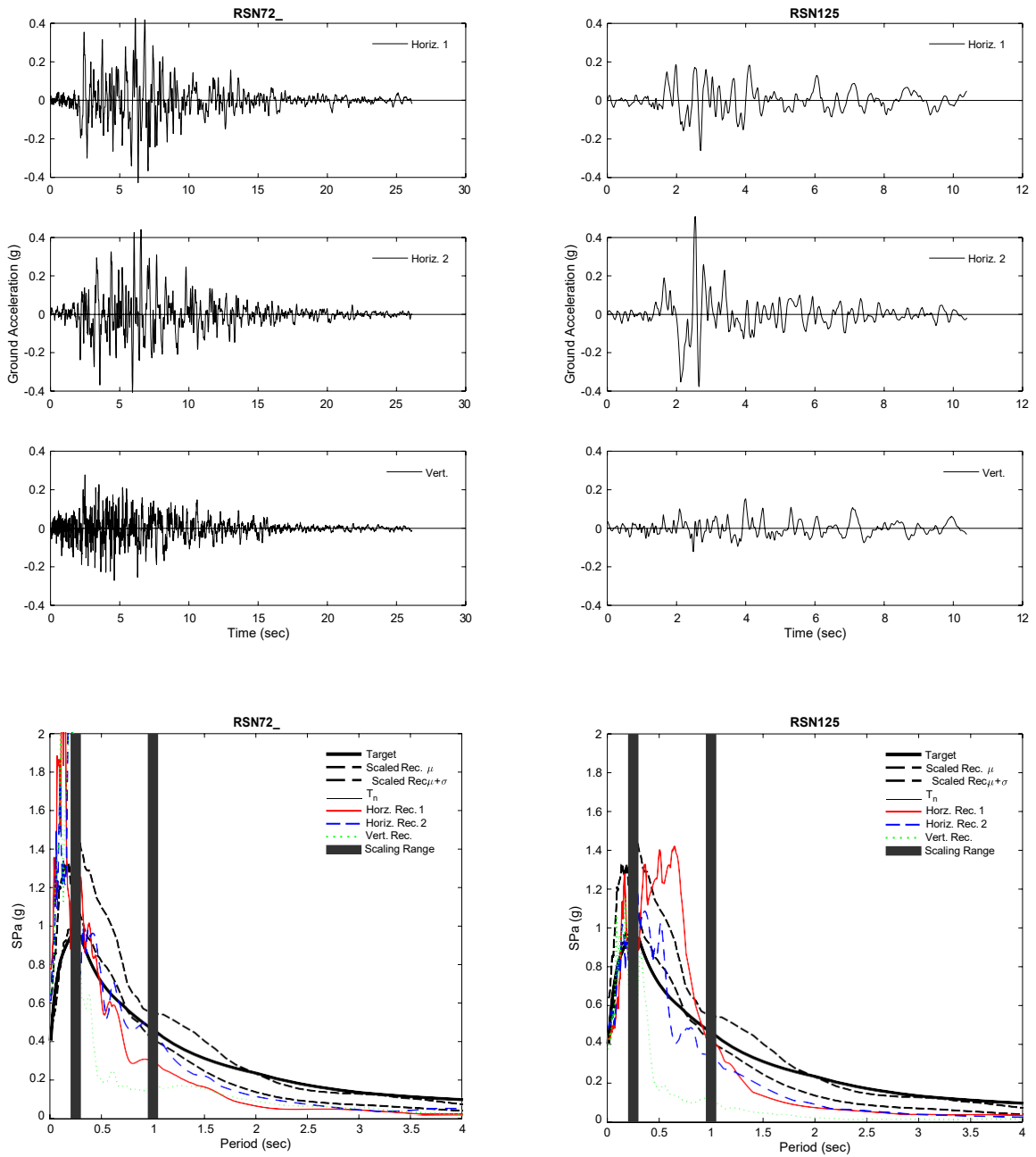


Figure A.1 Klamath River Bridge Ground Motion Scaled Suite Time Histories and Spectra (Continued)

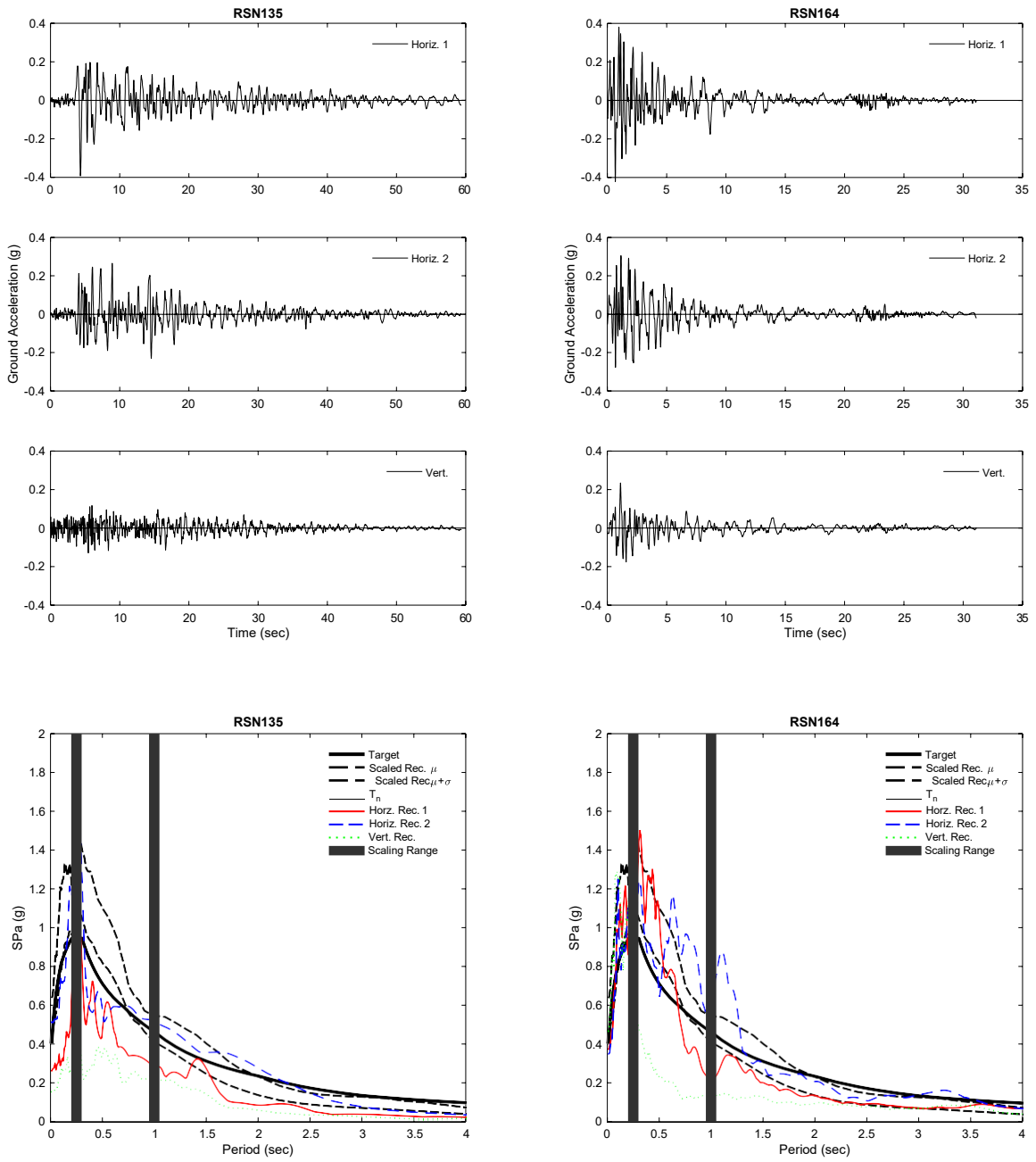


Figure A.1 Klamath River Bridge Ground Motion Scaled Suite Time Histories and Spectra (Continued)

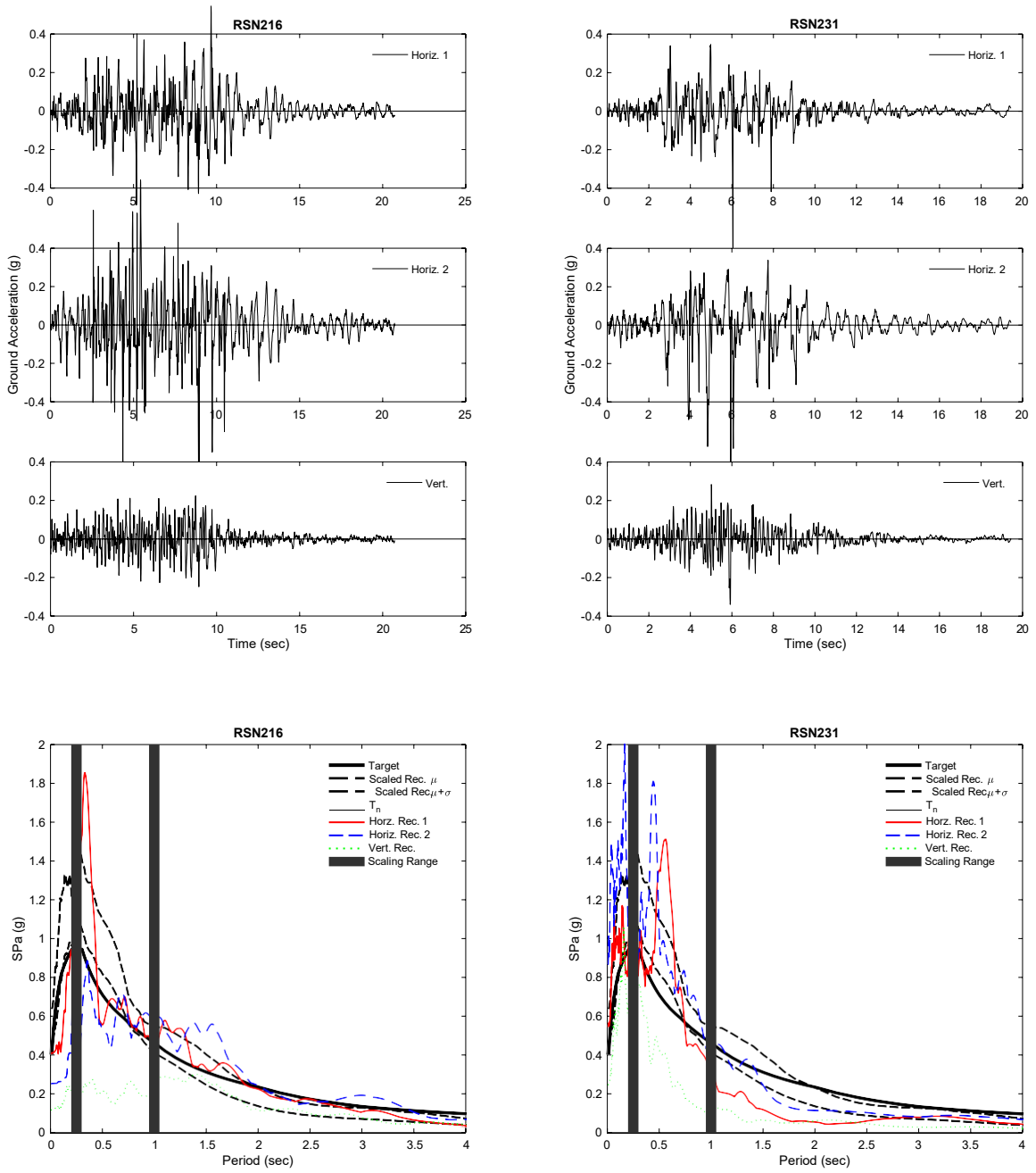


Figure A.1 Klamath River Bridge Ground Motion Scaled Suite Time Histories and Spectra (Continued)

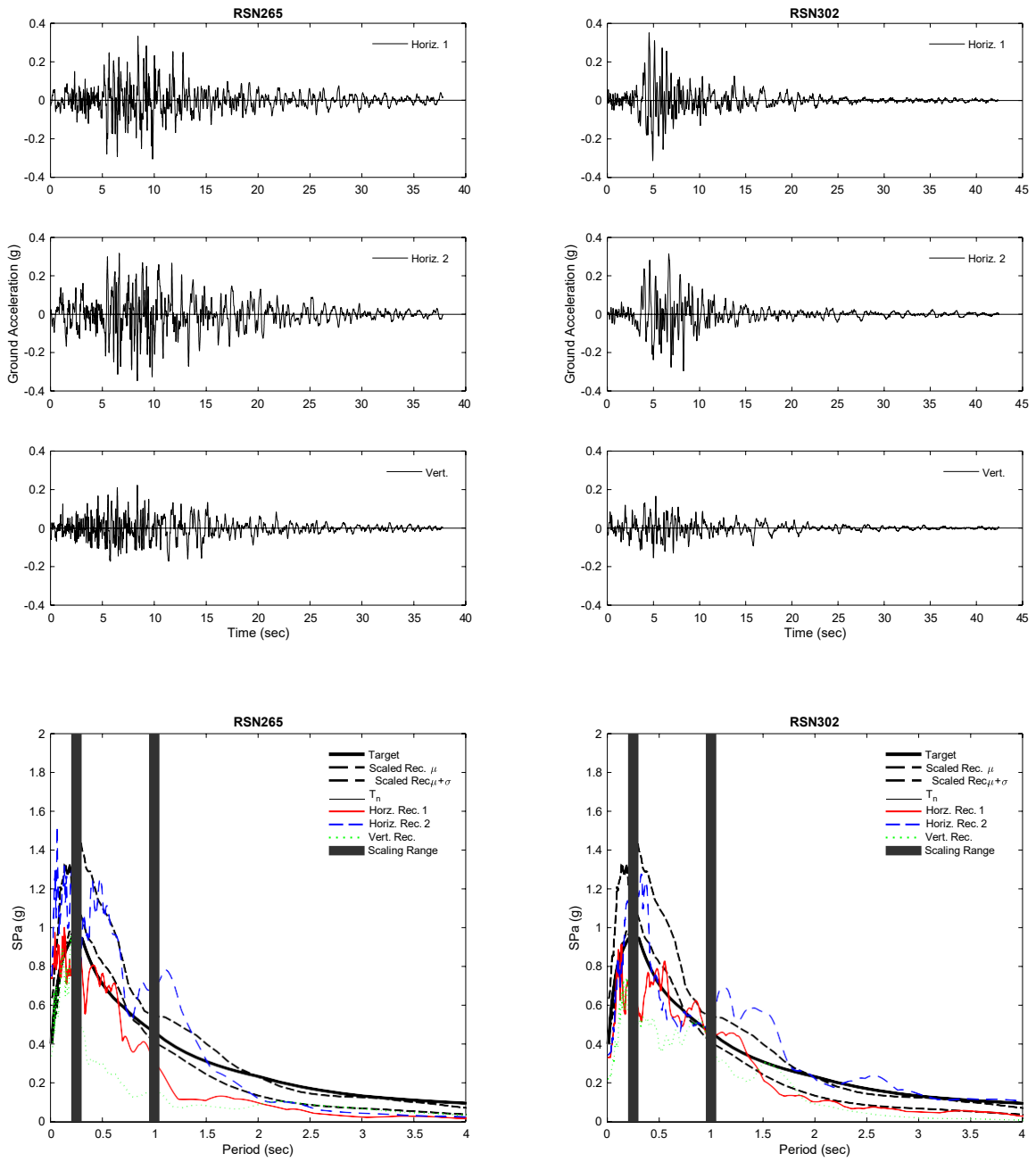


Figure A.1 Klamath River Bridge Ground Motion Scaled Suite Time Histories and Spectra (Continued)

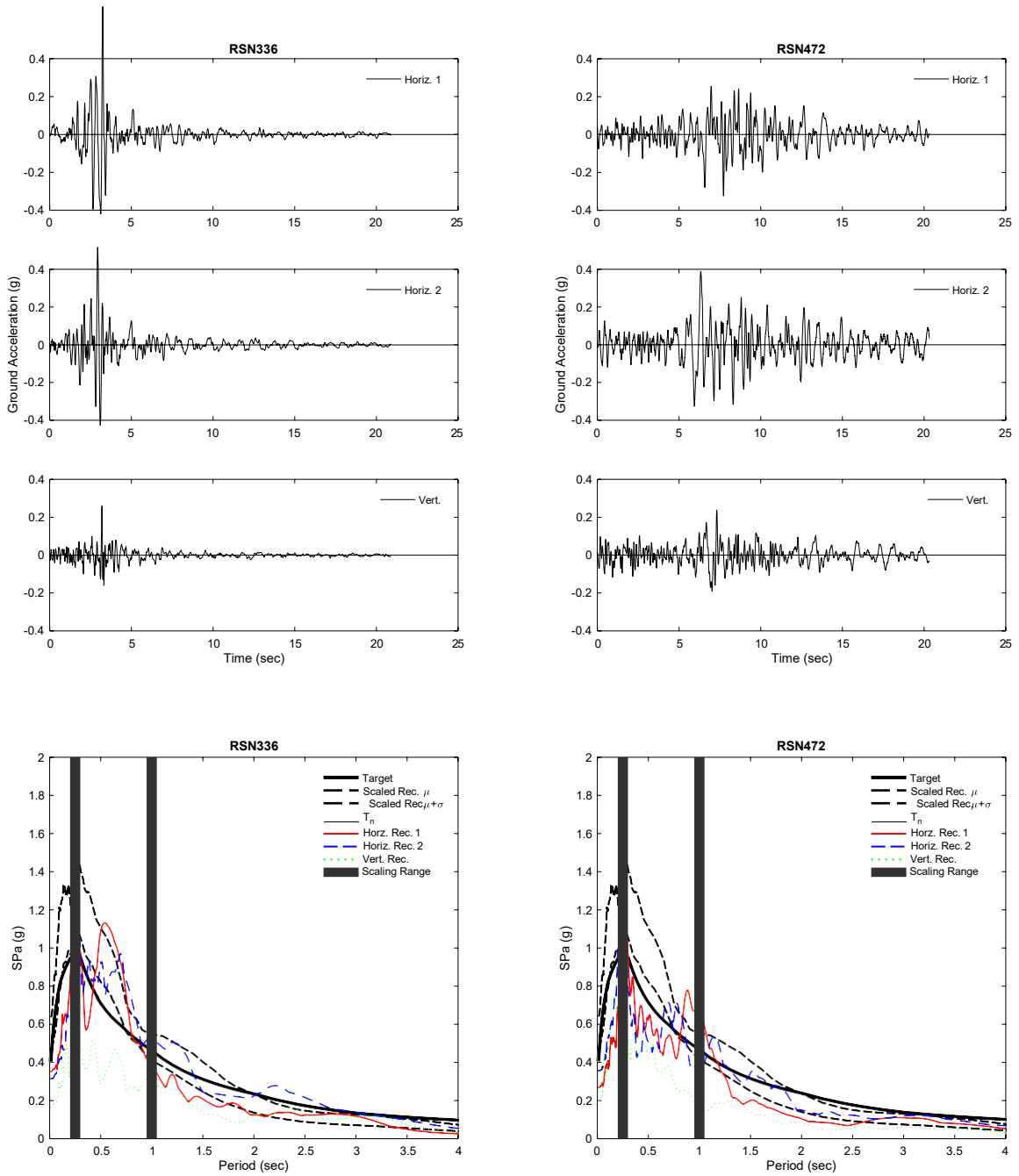


Figure A.1 Klamath River Bridge Ground Motion Scaled Suite Time Histories and Spectra (Continued)

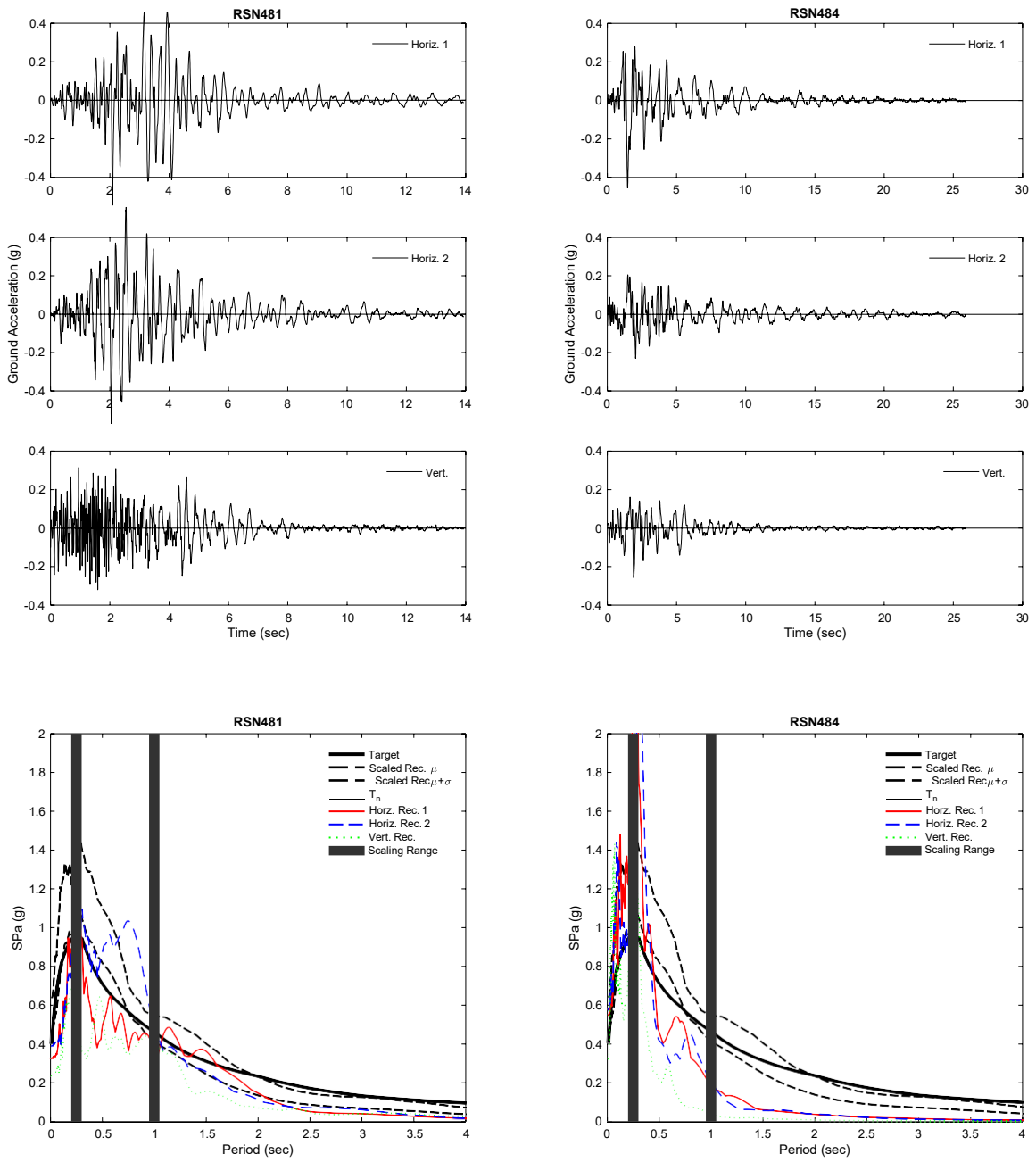


Figure A.1 Klamath River Bridge Ground Motion Scaled Suite Time Histories and Spectra (Continued)

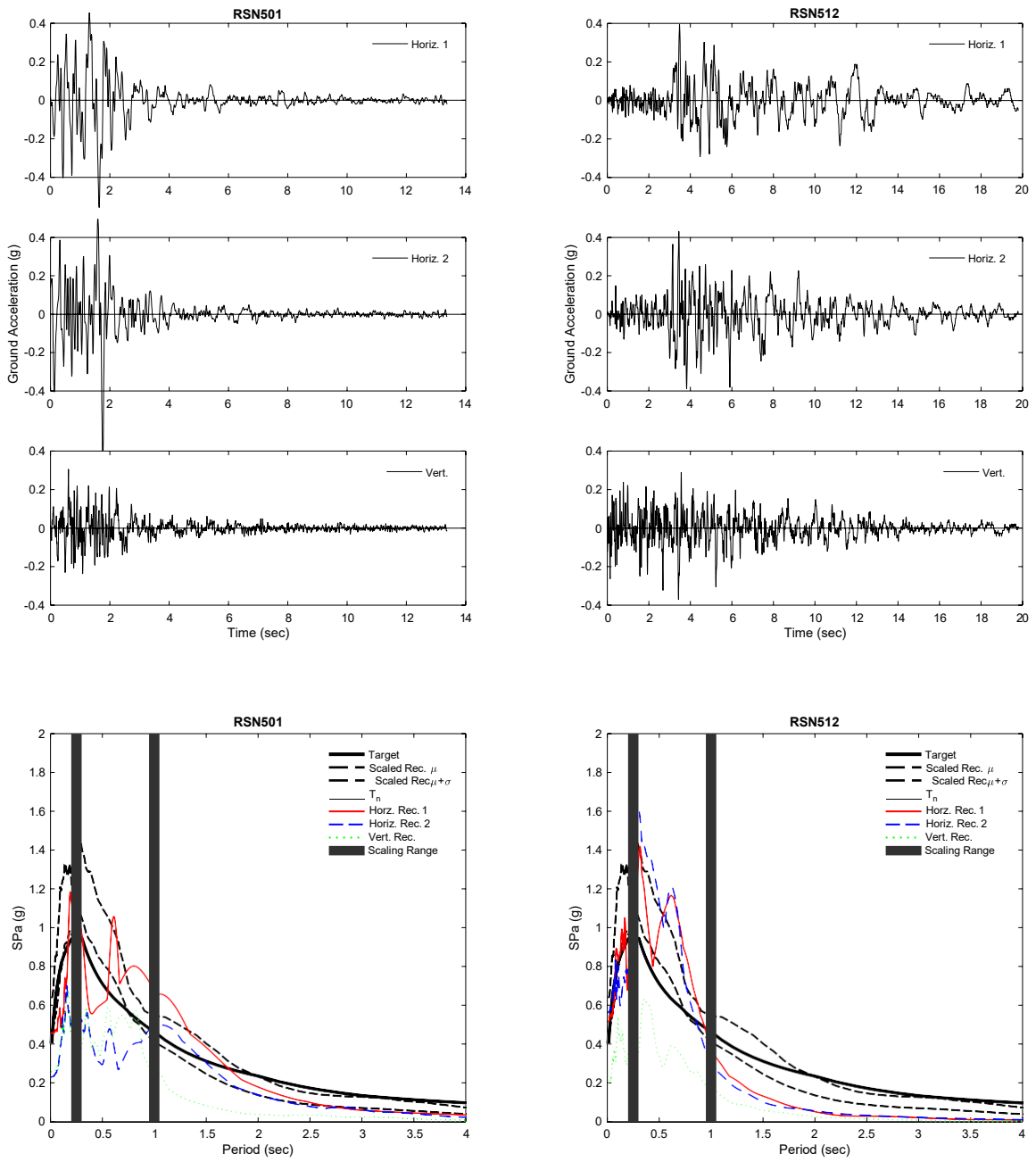


Figure A.1 Klamath River Bridge Ground Motion Scaled Suite Time Histories and Spectra (Continued)

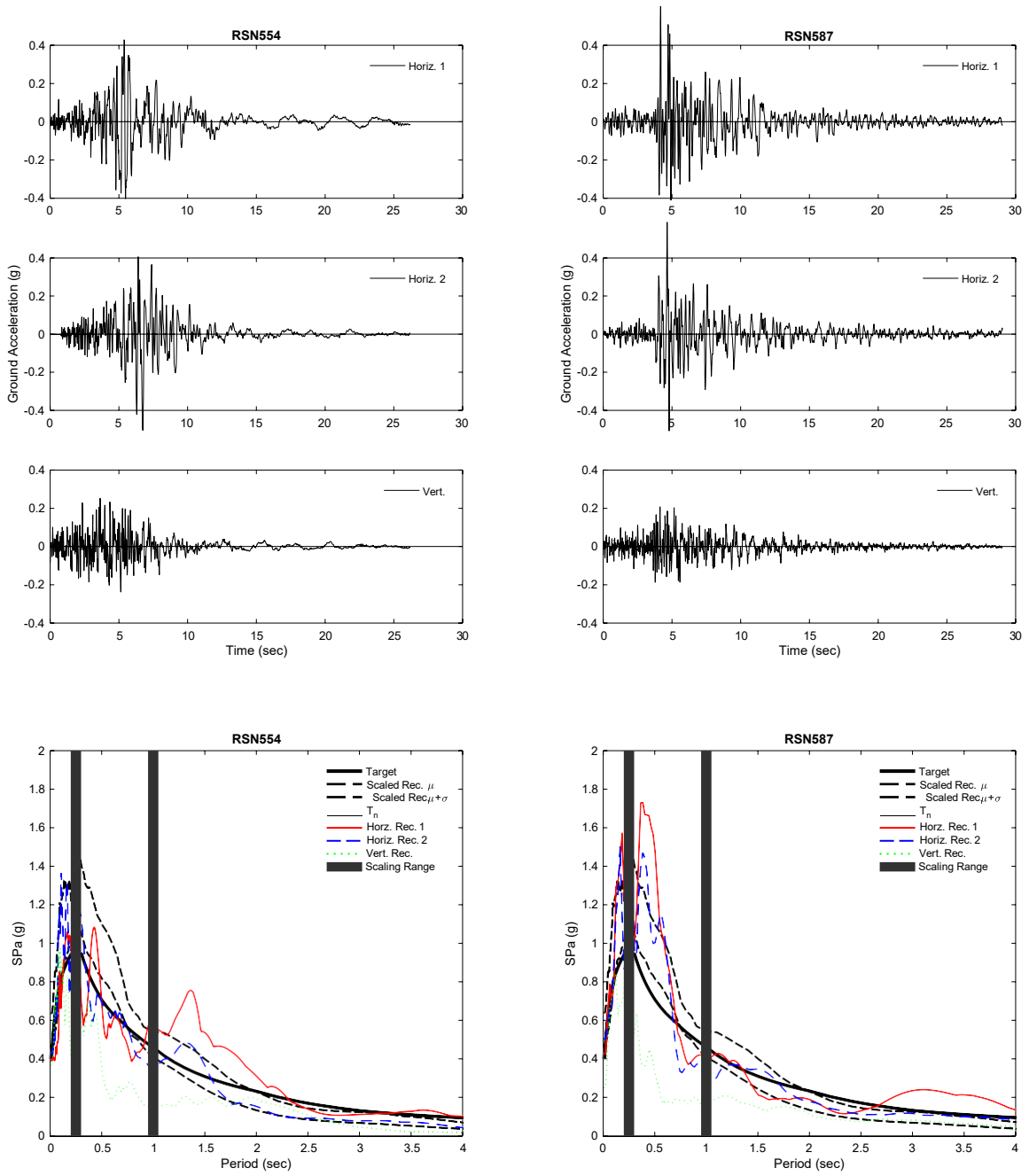


Figure A.1 Klamath River Bridge Ground Motion Scaled Suite Time Histories and Spectra (Continued)

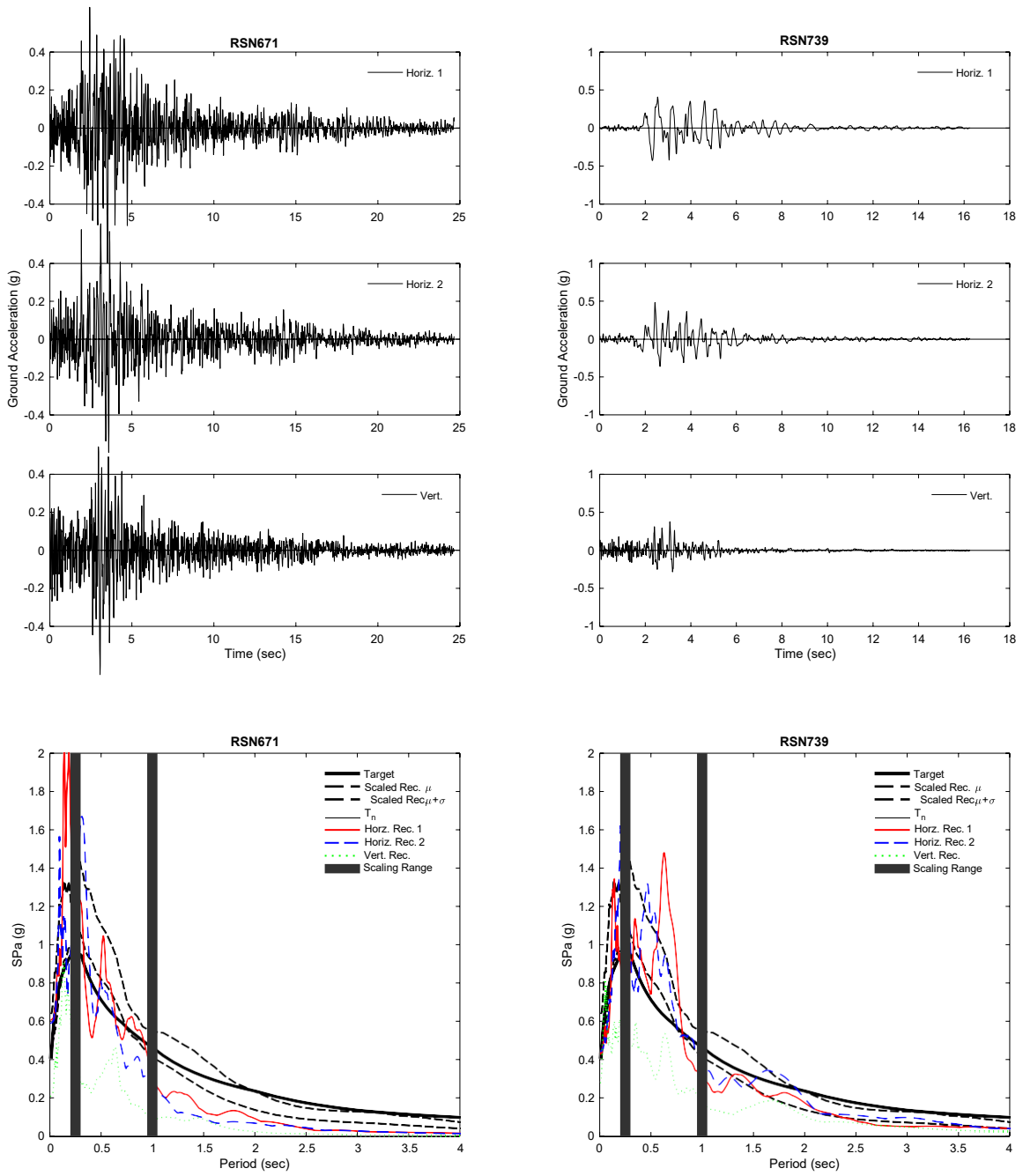


Figure A.1 Klamath River Bridge Ground Motion Scaled Suite Time Histories and Spectra (Continued)

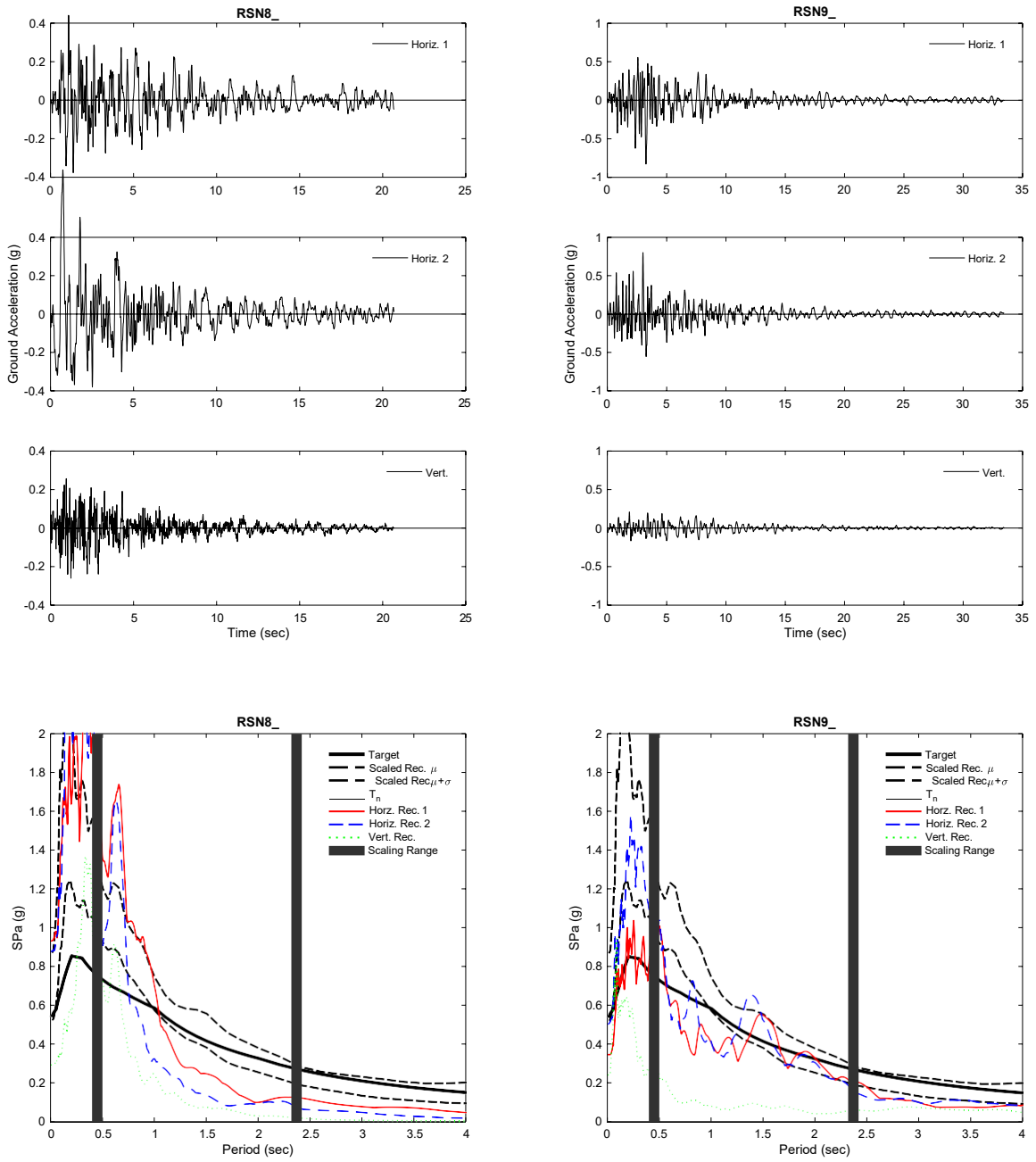


Figure A.2 San Luis Ray Bridge Ground Motion Suite Time Histories and Spectra

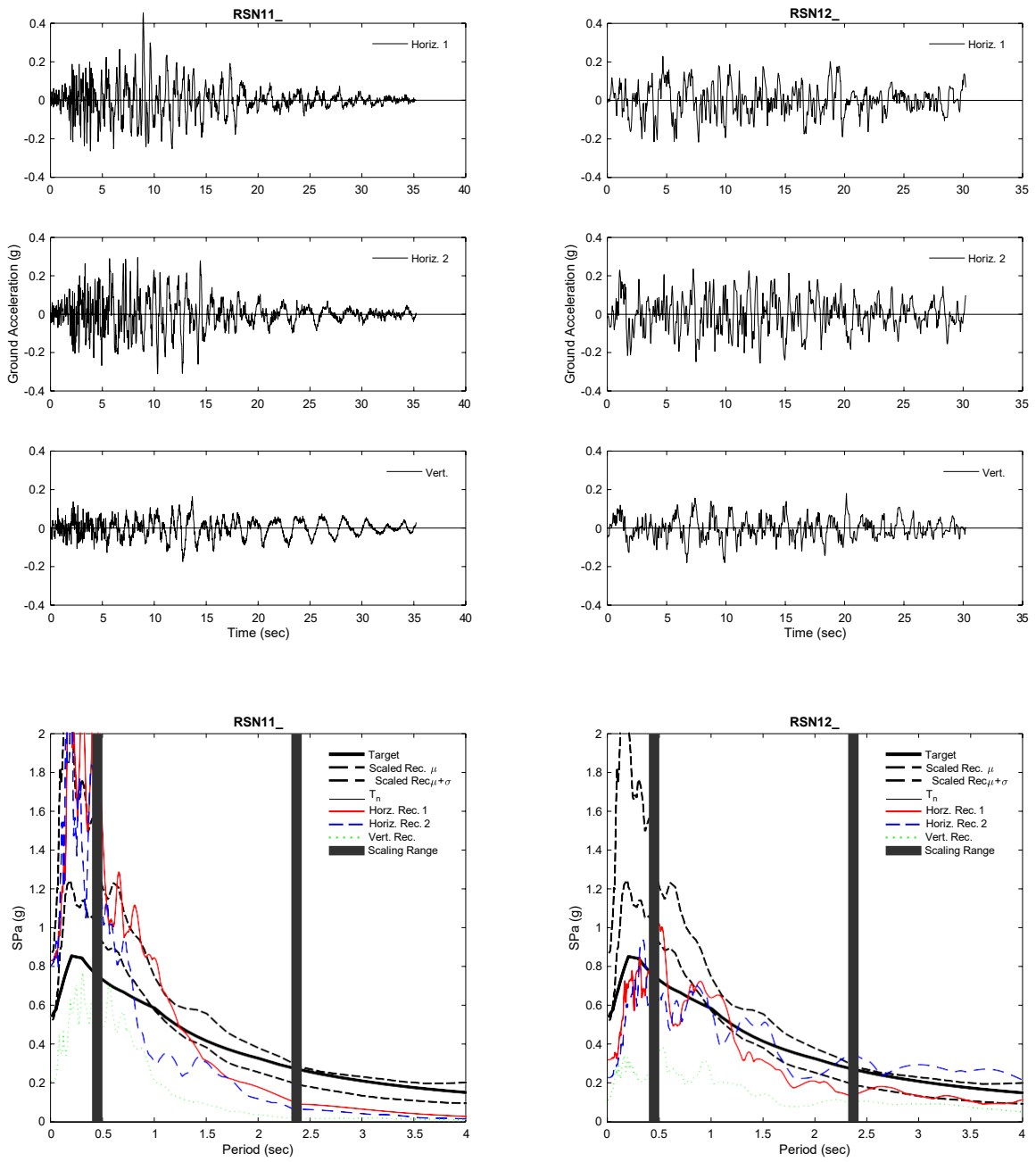


Figure A.2 San Luis Ray Bridge Ground Motion Suite Time Histories and Spectra (Continued)

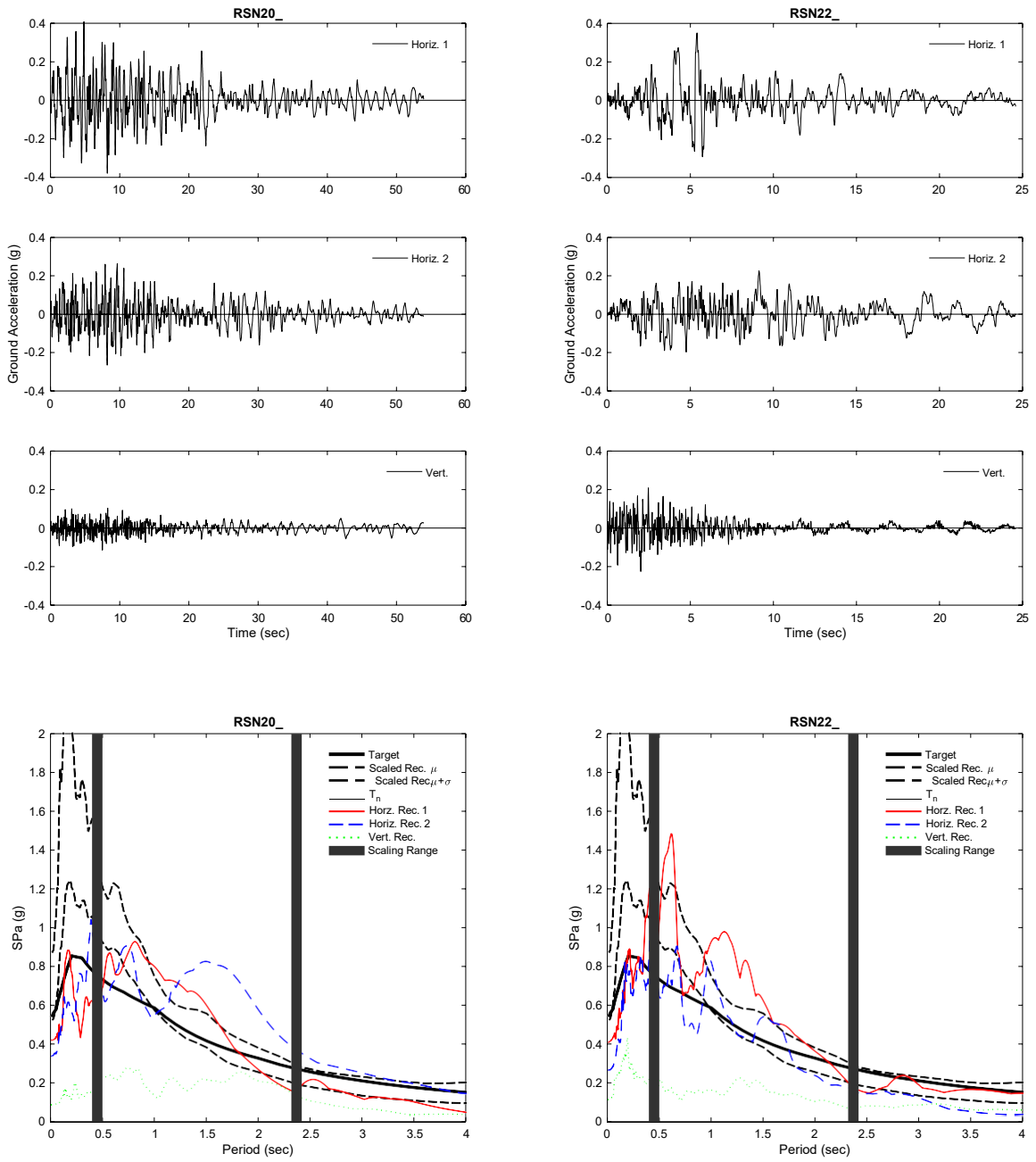


Figure A.2 San Luis Ray Bridge Ground Motion Suite Time Histories and Spectra (Continued)

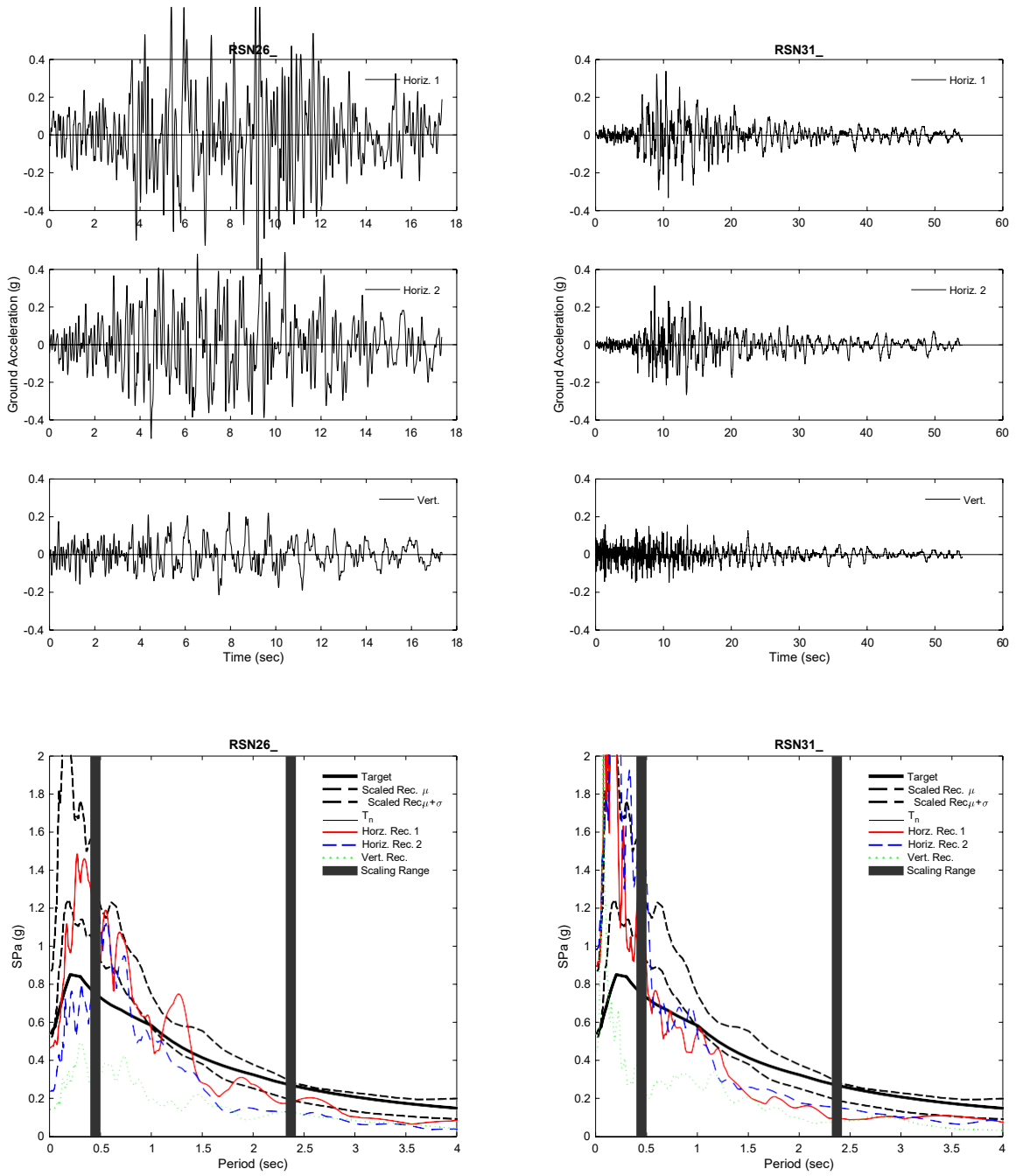


Figure A.2 San Luis Ray Bridge Ground Motion Suite Time Histories and Spectra (Continued)

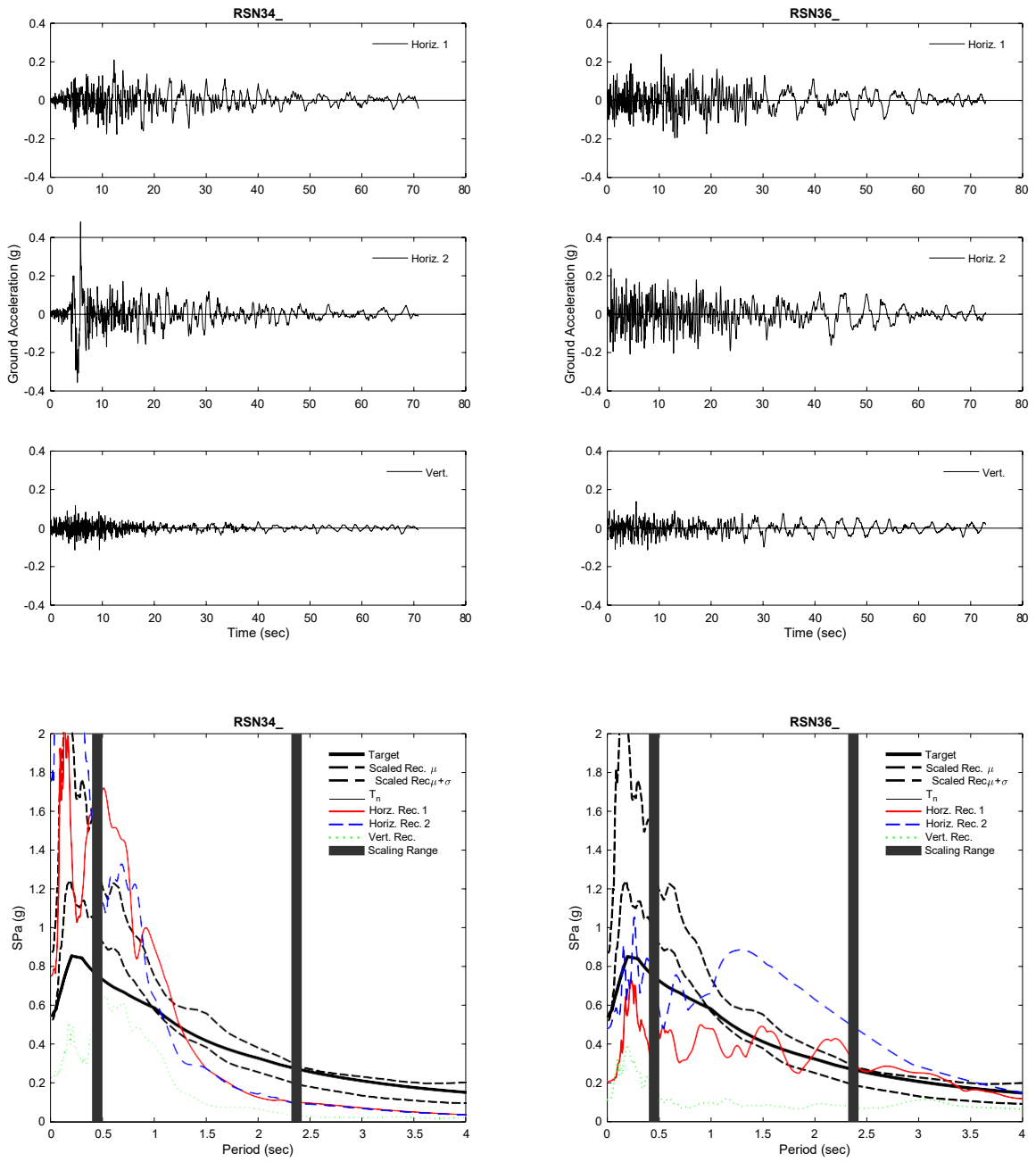


Figure A.2 San Luis Ray Bridge Ground Motion Suite Time Histories and Spectra (Continued)

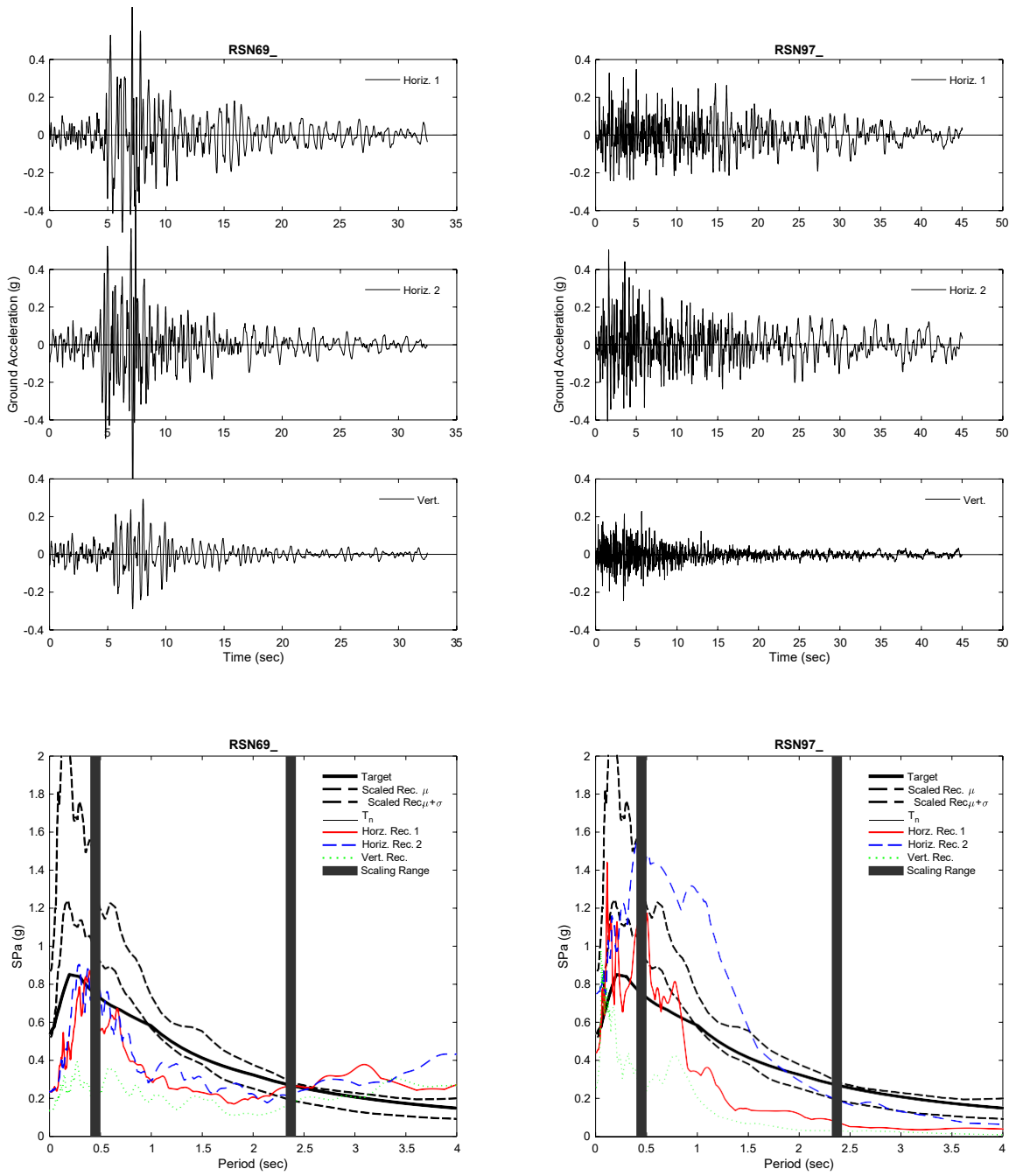


Figure A.2 San Luis Ray Bridge Ground Motion Suite Time Histories and Spectra (Continued)

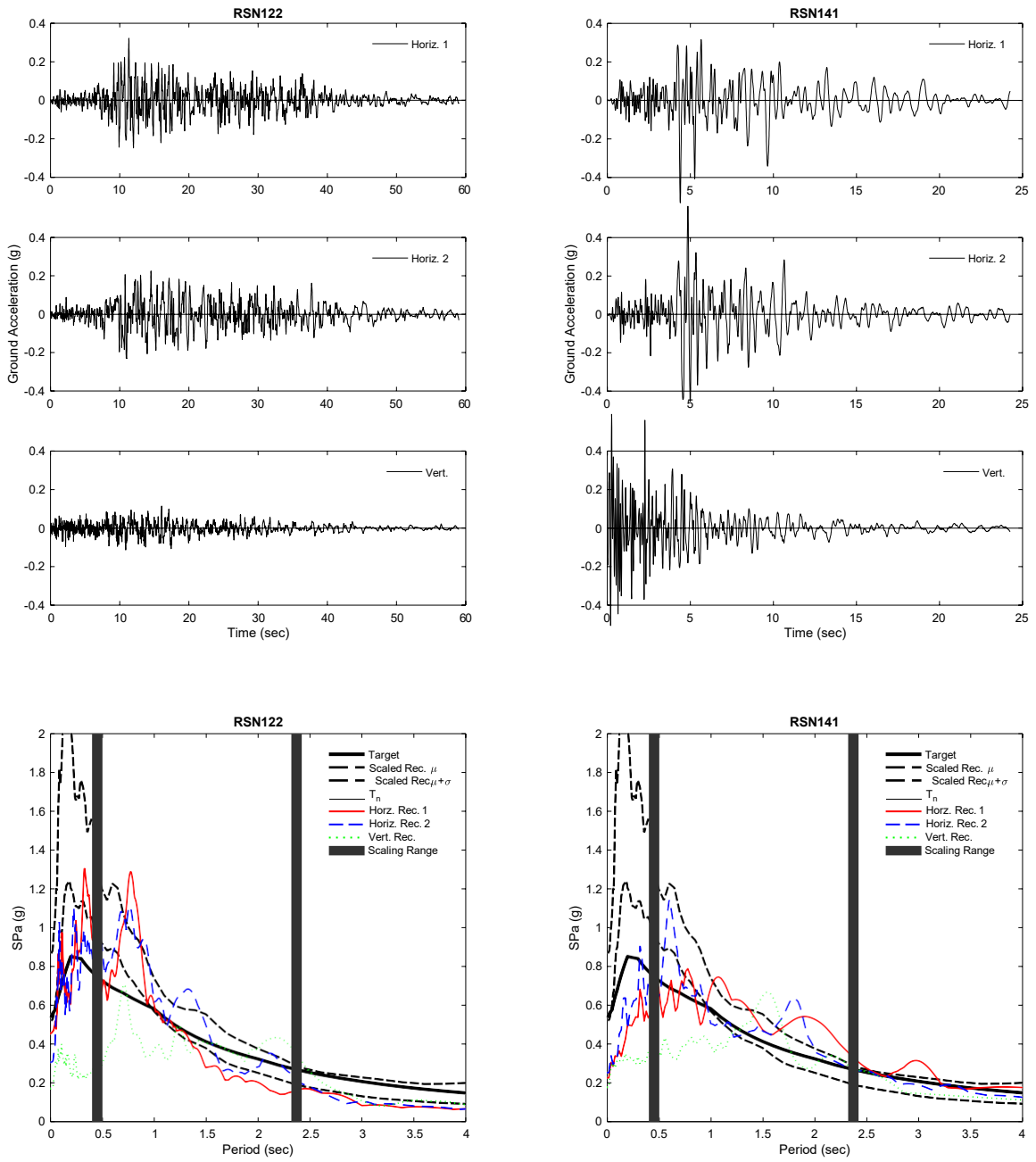


Figure A.2 San Luis Ray Bridge Ground Motion Suite Time Histories and Spectra (Continued)

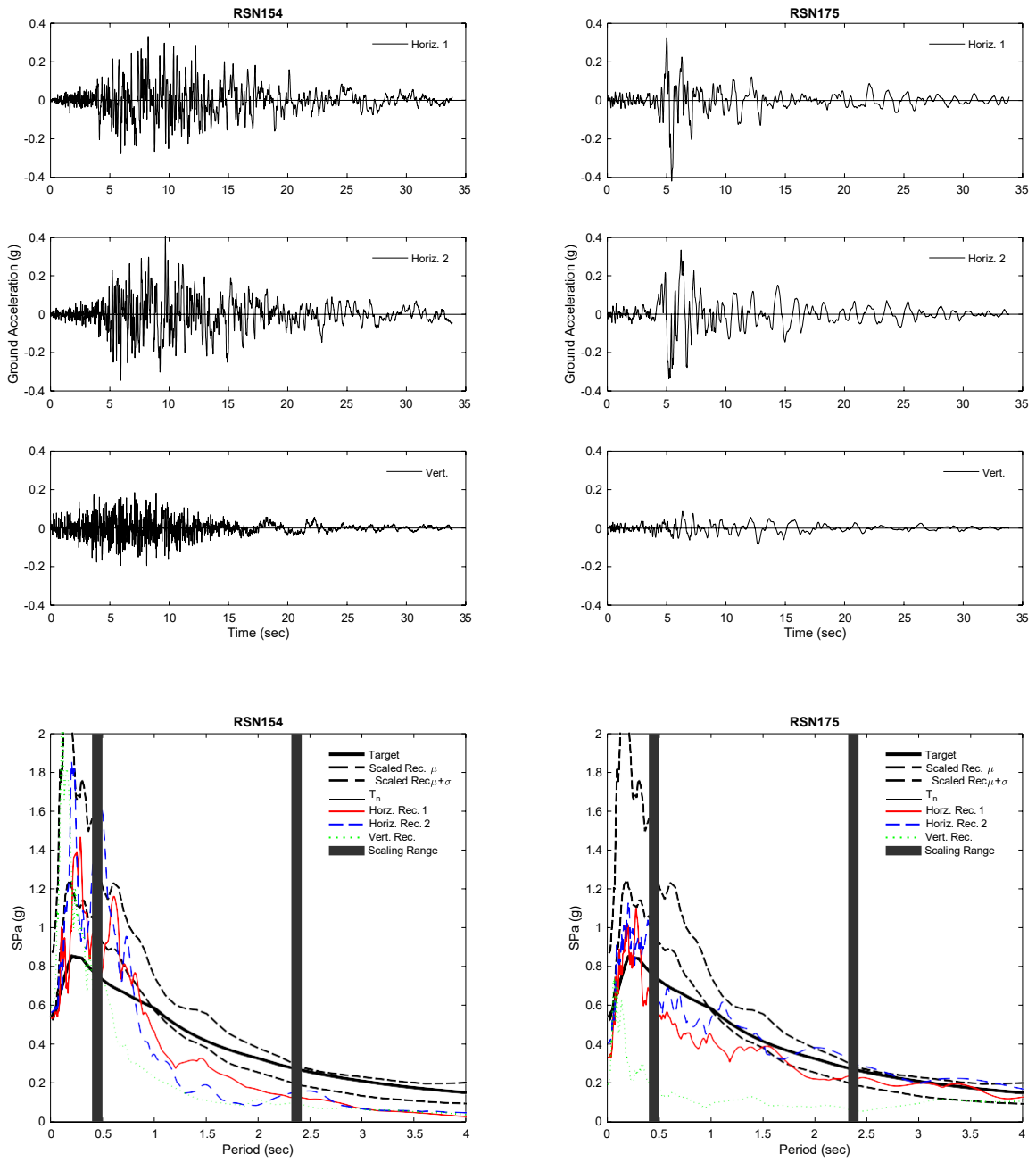


Figure A.2 San Luis Ray Bridge Ground Motion Suite Time Histories and Spectra (Continued)

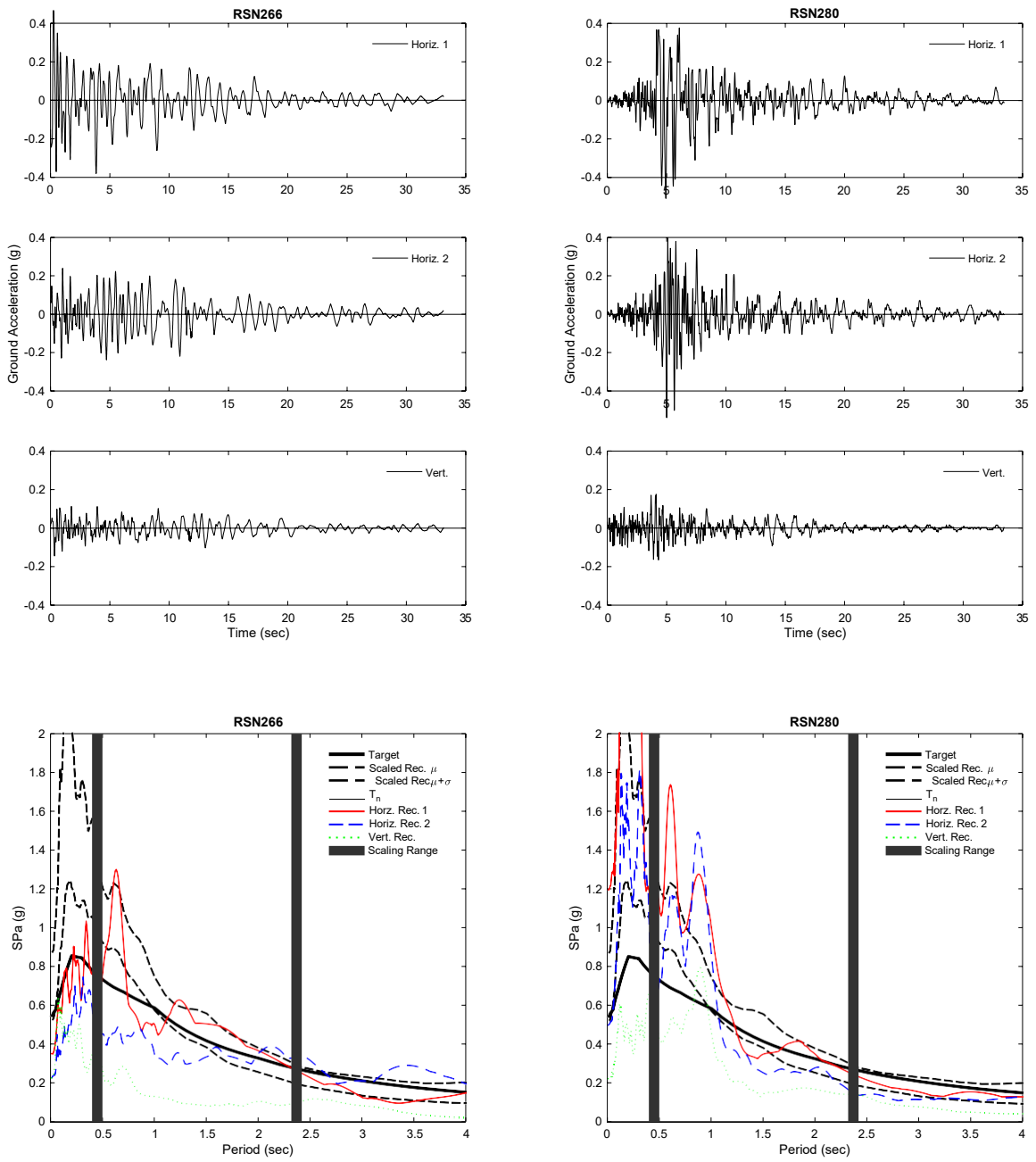


Figure A.2 San Luis Ray Bridge Ground Motion Suite Time Histories and Spectra (Continued)

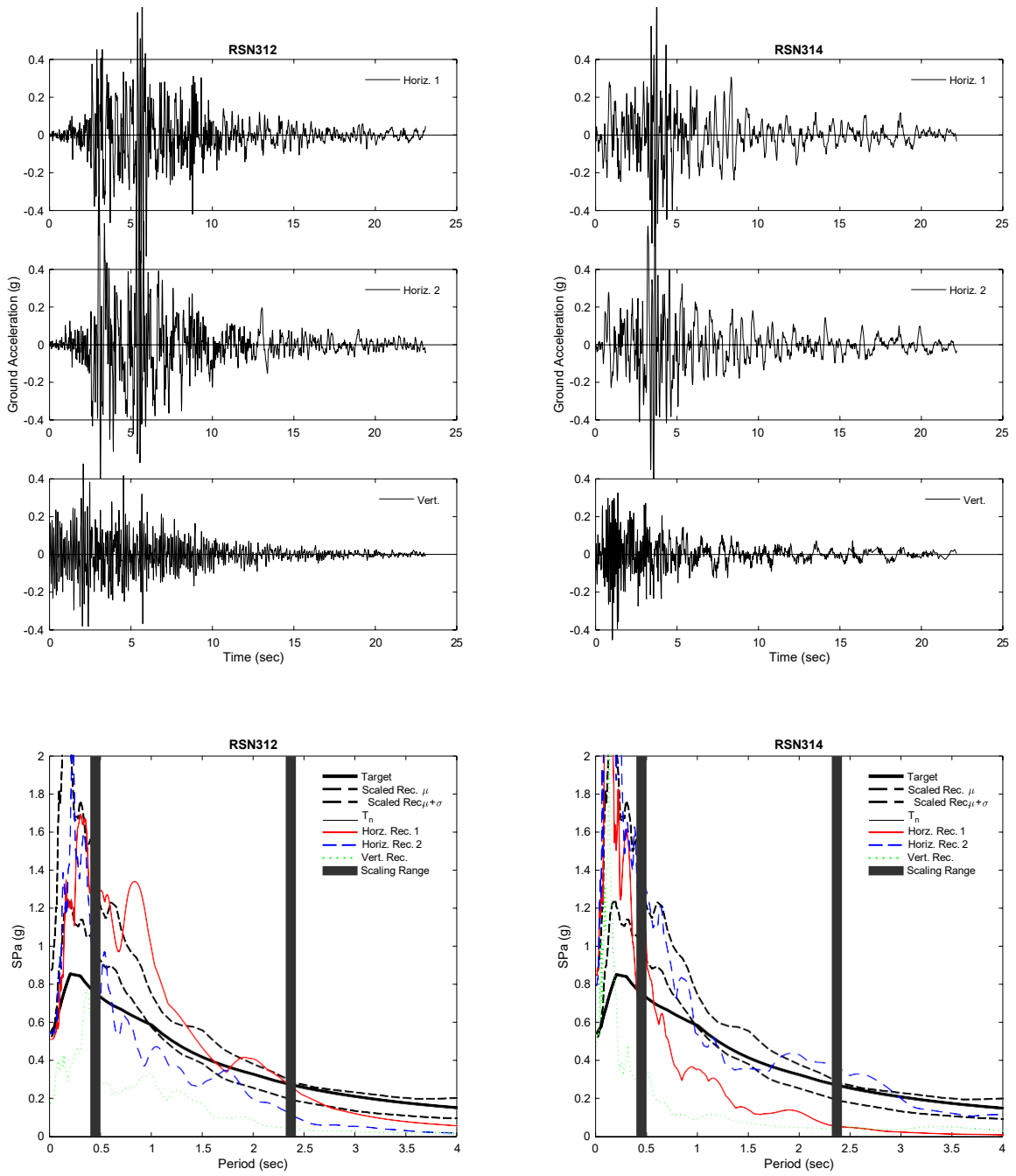


Figure A.2 San Luis Ray Bridge Ground Motion Suite Time Histories and Spectra (Continued)

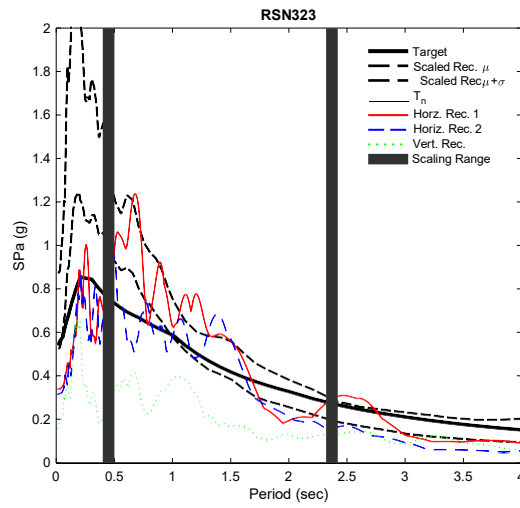
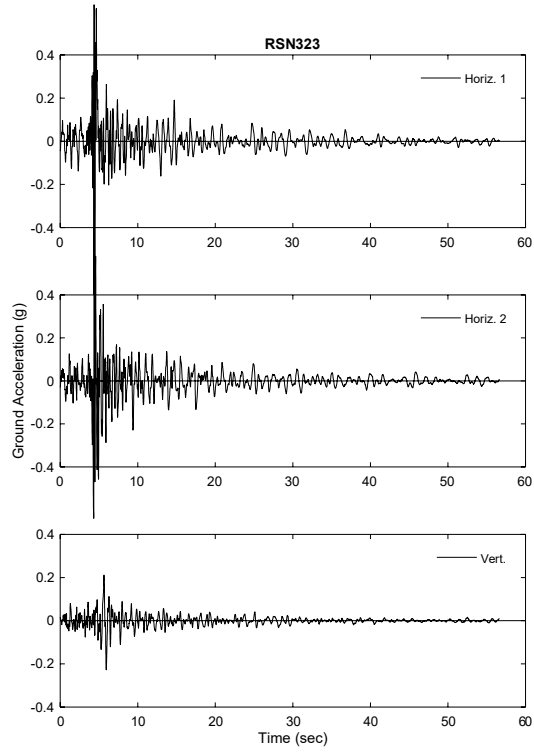


Figure A.2 San Luis Ray Bridge Ground Motion Suite Time Histories and Spectra (Continued)